

Modelling of atmospheric chlorine and
its effect on volatile organic
compounds

Peter Ivatt

MSc by Research

University of York

Chemistry

January 2017

Abstract

This study uses a recently developed halogen scheme (Sherwen et al., 2016) for the GEOSChem chemical transport model to perform an in-depth investigation into tropospheric atomic chlorine. In the study we find a global atomic Cl average concentration of 495 cm^{-3} with the highest concentrations of $1 - 5.5 \times 10^4 \text{ cm}^{-3}$ being located in the tropical marine boundary layer in tropical regions with a preference towards the north hemisphere. Globally the reaction between HOBr and HCl on sulfate aerosol dominates the production of Cl (77 %) precursors through its production of BrCl but in the boundary layer sea-salt sources through reaction with N_2O_5 or iodine species can dominate, particularly in polluted coastal regions. HCl is globally the dominant Cl_y species (80.9 %) but in the boundary layer other compounds (notably ClNO_2) can play a significant role. The rate of heterogeneous processing determines the ratio of HCl to more active Cl_y components. The model agrees with previous studies that Cl is a small sink compared to the OH sink (0.9 %). However, the Cl sink relative to the OH sink for ethane and propane is a more significant 15% and 6.5% respectively. There is a high degree of regional variability in the Cl removal of ethane, with the removal rising over the northern hemisphere oceans to ~50 % of OH removal at sea level and ~30 % averaged over whole column. Between 1998 and 2008 Cl concentrations increase globally due to developing regions experiencing increased Cl production due to increased concentration of pollutants NO_x and SO_4^{2-} and developed regions experiencing reduced loss due to decreases in NMVOC emissions. With the exception being Africa which as seen an increase in loss with minimal increase in production.

List of Contents

Chapter	Page
Abstract	2
List of Contents	3
List of Figures	5
List of Tables	9
Declaration	10
1. Introduction	11
1.1 Cl _y Release	11
1.1.1 Sea-Salt	11
1.1.2 Organic precursors	13
1.1.3 Stratospheric Source	13
1.2 Tropospheric Chlorine Species	13
1.3 VOC Oxidation	16
1.4 Aim of this Study	17
2. Model Description	19
2.1 Anthropogenic emissions	19
2.2 Halogen and sea-salt aerosol emissions	20
2.3 Chlorine chemistry scheme	21
2.4 Transportation and deposition	22
2.5 Simulations performed	22
3. Global Distribution of Atomic Chlorine	24
3.1 Sea level chlorine	24
3.2 Ground to 500 hPa	25
3.3 Ground to tropopause	26
3.4 Summary	28
4. Atomic Chlorine Sources	29
4.1 Cl production routes	29
4.2 BrCl	30
4.3 Sources of ClNO ₂	34
4.4 Sources from the decomposition of organic chlorine compounds	36
4.5 Sources from ICl photolysis	38
4.6 Summary	39
5. Chlorine Species and Cycling	40
5.1 Distribution of chlorine species	40
5.2 Cycling between species	45
5.3 Cl _y sinks	47
4.6 Summary	47
6. Atomic Chlorine Sinks and Atmospheric Oxidation	48

6.1 Cl removal routes	48
6.2 Removal of alkanes	50
6.3 Other VOCs	53
6.4 Summary	54
7. Chlorine Distribution Change 1988 to 2008	55
7.1 Emissions changes	55
7.2 Impact on non-halogenated species	59
7.2.1 Primary species	59
7.2.2 Secondary species	61
7.2.3 Halogenated species	63
7.3 Conclusions	64
8. Conclusion	66
9. References	67

List of Figures

Figures	Page
Figure 1.1 Generic representation of halogen chemistry in the atmosphere. In this case X=Cl and Y=other halogens (I, Br). Based on Wayne et al., 1995	14
Figure 1.2 shows, for a range of hydrocarbons, their rate constant for reaction with Cl divided by their rate constant for reaction with OH (at STP) (IUPAC).	16
Figure 3.1a (top) 3.1b (bottom) . 3.1a shows Cl concentration averaged over 2008 in molecules cm^{-2} from ground level to 589m altitude (the first 5 levels of GEOS-Chem). 3.1b shows Cl atoms integrated across each latitude.	24 – 25
Figure 3.2a (top) 3.2b (bottom) . 3.2a shows Cl concentration averaged over 2008 in Cl atoms cm^{-3} from ground level to the 500 hPa pressure level (the first 23 levels of GEOS-Chem). 3.2b shows Cl atoms averaged across each latitude.	25 – 26
Figure 3.3a (top), 3.3b (middle) and 3.3c (bottom) . 3.3a is the Cl concentration averaged over 2008 in Cl atoms cm^{-2} from ground level to tropopause, 3.3b is the Cl atoms averaged across each latitude. 3.3c is a zonal plot of Cl masked beyond the tropopause in Cl atoms cm^{-3} .	27
Figure 4.1 shows the zonal sea-level production of atomic Cl.	29
Figure 4.2 Average 2008 production of Cl atoms intergraded over the whole column averaged across each latitude.	30
Figure 4.3 Average 2008 production of Cl atoms $\text{cm}^{-3} \text{ s}^{-1}$ averaged for each vertical level.	30
Figure 4.4a (top) and 4.4b (bottom) . The average 2008 production of BrCl molecules in molecules $\text{cm}^2 \text{ s}^{-1}$ for sea level (4.4a) averaged across each latitude. The average 2008 cloud fraction (4.4b) at sea level.	31 – 32
Figure 4.5a (top) ,4.5b (middle) and 4.5c (bottom) The average 2008 production of BrCl molecules in molecules $\text{cm}^2 \text{ s}^{-1}$ for whole column (4.5a) averaged across each latitude. BrCl production averaged over each vertical level of the model (4.5b). The average 2008 cloud fraction (4.5c) at sea level.	33

Figure 4.8a (Top) and 4.8b (Bottom). Cl concentration due to the inclusion of ClNO ₂ in the simulation, sea level (4.8a) and whole column (4.8b).	34 – 35
Figure 4.9 Average 2008 production of Cl atoms for sea level averaged across each latitude between -5 and 20 degrees' longitude.	35
Figure 4.10a (top) and 4.10b (bottom). The average 2008 production of Cl atoms cm ⁻² s ⁻¹ from organic chlorine (4.10a) and OH concentration (4.10b) at sea level averaged across each latitude.	36
Figure 4.11a (top) and 4.11b(bottom). The average 2008 production of Cl atoms cm ⁻² s ⁻¹ from organic chlorine (4.11a) and OH concentration (4.11b) for whole column averaged across each latitude.	37
Figure 4.12a (top), 4.12b (middle) and 4.12c (top) The average 2008 production of ICl molecules for sea level (4.12a) and whole column (4.12b) averaged across each latitude. 4.12c is the production of ICl molecules averaged over each vertical level.	38 – 39
Figure 5.1 Concentrations of (from top to bottom) Cl _y , HCl, BrCl, ClNO ₂ and ICl. Sea level concentration are on the left with whole column averages on the right.	40 – 41
Figure 5.2 Concentrations of (from top to bottom) Cl _{cycling} , HOCl, ClNO ₃ , and ClO _x . With sea level on the left and whole column average on the right.	42 – 43
Figure 5.3a (top) and 5.3b (bottom) Figure 5.3 shows the speciation of Cl species in a zonal form at the surface (a) and averaged through the column (b).	44
Figure 5.4 Lifetime of (from top to bottom) Cl, Cl _y and ClO _x . With sea level on the left and whole column average on the right. The fast cycling between Cl and O ₂ to form ClOO has been excluded from the Cl the lifetimes calculated here.	45 – 46
Figure 6.1 shows the zonal mean rate of loss of atomic Cl by reaction with VOCs at sea-level.	48
Figure 6.2a(top) and 6.2b(bottom) whole column zonal plot loss of atomic Cl(a), plot of loss by altitude(b).	49
Figure 6.3a (top) and 6.3b (bottom) the zonal average Cl and OH concentrations and the ratio, both at the surface (a) and through the column (b).	50

Figure 6.4a-b (top), c-d (middle) and e-f (bottom) shows the zonally averaged removal sea-level (left) and whole column (right) methane (top), ethane (middle) and propane (bottom).	51
Figure 6.5a (top) and b (bottom) C ₂ H ₆ removal via Cl as % of OH at sea level (a) and averaged over the column (b)	52 – 53
Figure 6.6 Comparison of VOC removal via OH and Cl, averaged over sea level (left column) and whole column (right column).	53
Figure 7.1 NO emissions in 1988 (top left) 2008 (top right) and the change in percentage (left).	55 – 56
Figure 7.2 CO emissions in 1988 (top left) 2008 (top right) and the change in percentage (left).	56
Figure 7.3 SO ₂ emissions in 1988 (top left) 2008 (top right) and the change in percentage (left).	56 – 57
Figure 7.4 C ₂ H ₆ emissions in 1988 (top left) 2008 (top right) and the change in percentage (left).	57
Figure 7.5 C ₃ H ₈ emissions in 1988 (top left) 2008 (top right) and the change in percentage (left).	57 – 58
Figure 7.6 Combined CH ₂ O, acetone, C ₄ + alkanes and acetaldehyde emissions in 1988 (top left) 2008 (top right) and the change in percentage (left).	58
Figure 7.7 CO whole column average concentration in 1988 (top left) 2008 (top right) and the change in percentage (left).	59
Figure 7.8 NO _x whole column average concentration in 1988 (top left) 2008 (top right) and the change in percentage (left).	60
Figure 7.9 SO ₄ ²⁻ whole column average concentration in 1988 (top left) 2008 (top right) and the change in percentage (left).	60
Figure 7.10 C ₂ H ₆ whole column average concentration in 1988 (top left) 2008 (top right) and the change in percentage (left).	61
Figure 7.11 C ₃ H ₈ whole column average concentration in 1988 (top left) 2008 (top right) and the change in percentage (left).	61
Figure 7.12 OH whole column average concentration in 1988 (top left) 2008 (top right) and the change in percentage (left).	62
Figure 7.13 O ₃ whole column average concentration in 1988 (top left) 2008 (top right) and the change in percentage (left).	62 – 63

Figure 7.14 Cl_{cycling} whole column average concentration in 1988 (top left) 2008 (top right) and the change in percentage (left). 63 – 64

Figure 7.15 atomic Cl whole column average concentration in 1988 (top left) 2008 (top right) and the change in percentage (left). 65

List of Tables

Figures	Page
Table 2.1 How EDGAR emission used in the simulation are handled by the Harvard-NASA emissions component (HEMCO)	19
Table 2.2 EMEP sector assigned to each EDGAR sector for speciation	19
Table 2.3 How the halogen emissions used in the simulation are handled by the Harvard-NASA emissions component (HEMCO)	20

Declaration

I declare that this thesis is a presentation of original work and I am the sole author.
This work has not previously been presented for an award at this, or any other,
University. All sources are acknowledged as References.

1. Introduction

The chemistry of the troposphere plays a central role in determining many societal problems such as climate change and air quality. The chemistry in the troposphere is one of oxidation where primary pollutants are emitted into the atmosphere and are then oxidized to the point where they can be deposited back to the surface. The oxidizing agent in the atmosphere have historically been through to be dominated by OH with O₃, NO₃ and H₂O₂ playing roles in some specific environments (Atkinson 2000).

The OH radicals effect on the troposphere has been study extensively over previous decades, however another radical which has been largely ignored which could potentially be having profound effects on the troposphere is atomic Cl (Finlayson-Pitts 1989) The lack of investigation is down to the difficulty of directly measuring atomic Cl due to its incredibly short concentration. Current predictions for the atomic Cl concentration are wildly different from 10² cm⁻³ based on analysis of VOC ratios (Wingenter 1999) to 10⁵ cm⁻³ based on Cl family detection (Keene et al., 2007).

This chapter describes what is thought to be the dominant chemical processes by which reactive chlorine is released into the atmosphere, it is processed in the atmosphere in to various inorganic chlorine compounds and is finally deposited back to the surface.

1.1 Cl_y release

Reactive chlorine (inorganic chlorine which is capable of being in the gas phase, notably excluding aerosol phase chloride) is released into the troposphere in multiple mechanisms. The dominant is the conversion of predominantly sea-salt chloride into Cl_y (Graedel and Keene 1996) but also from organic precursor gases and from the stratosphere.

1.1.1 Sea-salt

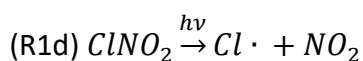
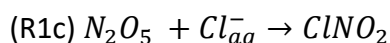
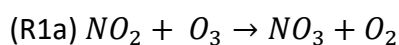
Sea salt aerosol released from ocean is the predominant source of inorganic tropospheric chlorine (Graedel and Keene 1996). Sea salt aerosol is produced by air bubbles bursting in the ocean as a result of wind stress (Jaeglé et al., 2011) this releases vast amounts of material into the atmosphere. Large droplets have a very short lifetime in the atmosphere as they rapidly return to the ocean. However,

smaller droplets may have a long enough lifetime (mins- hours) to allow it transported through the boundary layer and so form part of the atmospheric system.

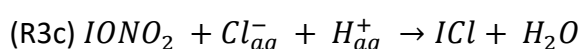
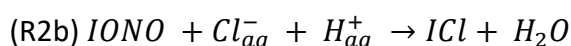
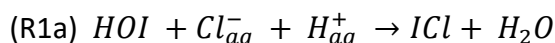
Sea-water and so sea-salt aerosol made up of a complex mixture of inorganic and organic components (O'Dowd et al., 2004) with chloride being a significant fraction of the overall mass.

Releasing this chloride from the aerosol phase into the gas phase is difficult but can be achieved through a range of reactions where gas phase species ab/adsorb onto the aerosol and undertake a set of chemical reactions releasing gas phase inorganic chlorine species.

The ability of N_2O_5 to uptake onto aerosol to subsequently release nitryl chloride ($ClNO_2$) has been known for some time (Finlayson-Pitts 1989). However, it has only been in the last decade as instruments have advanced that the signature of this route to produce reactive chlorine has been evident both in polluted marine regions which concentrations of sea-salt and NO_x are high and in continental regions where NO_x is high but the source of chloride is less certain (Osthoff et al., 2008, Thornton et al., 2010 and Sarwar et al., 2014). Atomic Cl is produced from $ClNO_2$ via the mechanism:

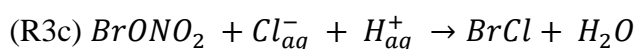
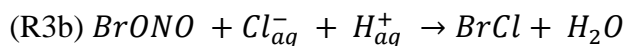
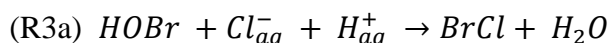


Other mechanisms exist for releasing reactive chlorine compounds into the gas phase. The next most significant is thought to be through inter-halogen reactions. For example, scavenging of the iodine species HOI , INO_2 , and $IONO_2$ by sea salt aerosol particles results in aqueous-phase chemical reactions that can produce the compound ICl which will be released back into the gas phase due to its low solubility (Vogt et al., 1999). The three production mechanisms for ICl are:



A similar activation mechanism on sea salt aerosol may also occur whereby $HOBr$ which is scavenged by sea salt aerosol can rapidly react with Cl^- to produce $BrCl$.

BrCl is only slightly soluble and escapes to the gas phase where they rapidly undergo photolysis (Vogt et al., 1996).



1.1.2 Organic precursors

A range of chlorine compounds are emitted into the atmosphere (WMO 2014). Some of these compounds (e.g. CFCs) are effectively inert in the troposphere as they cannot decompose either by a chemical oxidant or by photolysis. However, some of these can be oxidized in the atmosphere to release Cl either by reaction with OH or photolysis. The most abundant organic chlorine sources in the troposphere are CH₃Cl, CH₂Cl₂ and CHCl₃ (Ordóñez et al., 2012). There is currently some debate about what fraction of this organic chlorine become reactive chlorine due to deposition of intermediate compounds (Hossaini et al., 2016).

1.1.3 Stratospheric source

Although compounds such as CFC cannot be decomposed in the troposphere they may decompose in the stratosphere where UV light is more intense (WMO, 2014). The reactive chlorine released in this way must ultimately return to the surface. Thus a flux of reactive chlorine from the stratosphere into the troposphere must exist (Sherwen et al., 2016). The magnitude of this source and the speciation though is highly uncertainty.

1.2 Tropospheric chlorine species

Once released into a reactive form chlorine compounds may undertake a complex chemistry. Until ultimately being converted into a form (typically HCl) where it can be deposited to the surface. Compounds in this class include Cl₂, HCl, BrCl, ClO, HOCl, ClNO₂ and ClNO₃. Figure 1.1 Shows this chemistry diagrammatically

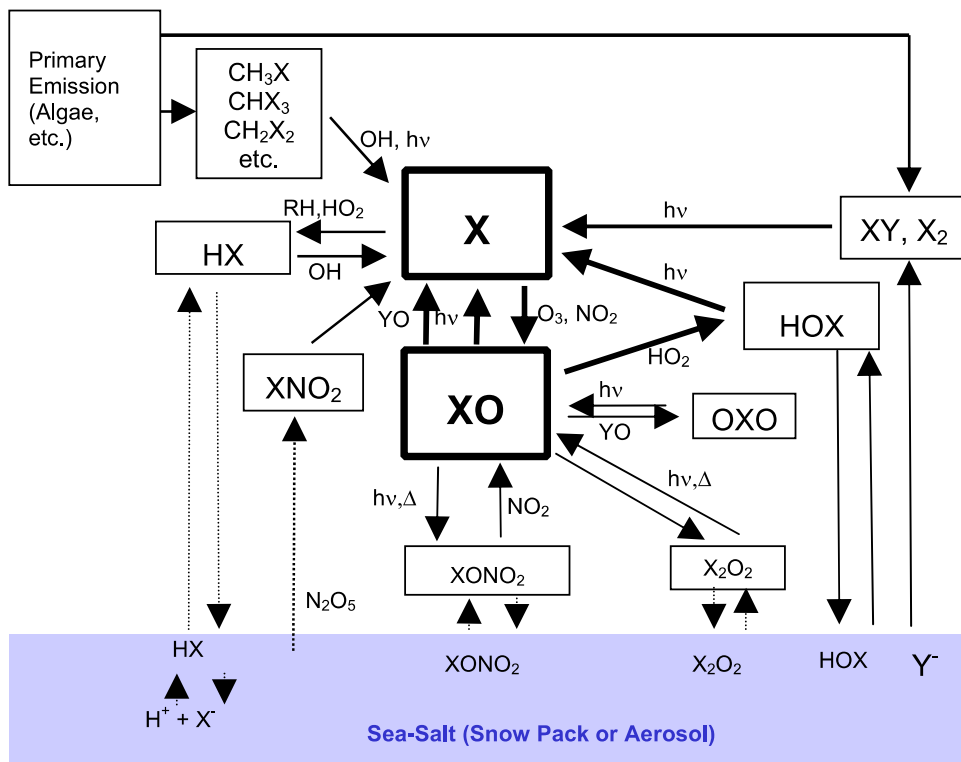
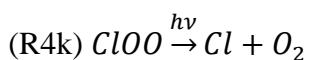
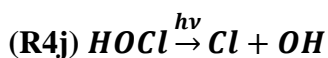
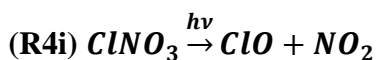
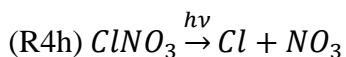
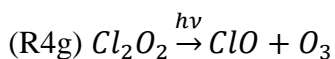
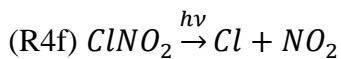
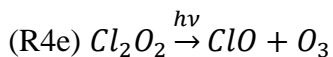
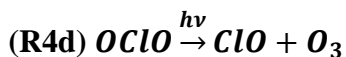
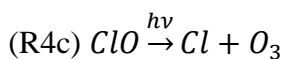
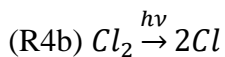
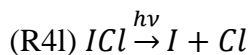


Figure 1.1 Generic representation of halogen chemistry in the atmosphere. In this case X=Cl and Y=other halogens (I, Br). Based on Wayne et al., 1995

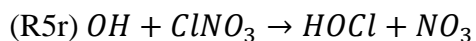
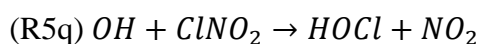
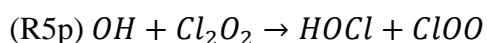
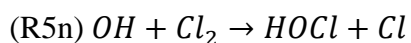
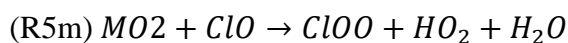
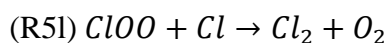
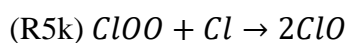
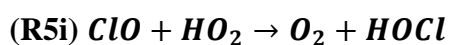
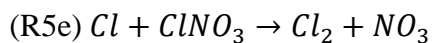
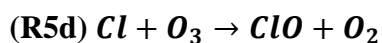
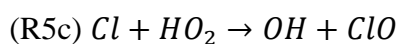
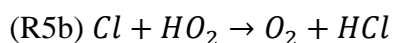
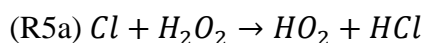
Interconversion (cycling reactions) between these Cl_y species in the troposphere can occur via the following reactions (with the key reactions that flux in excess of 1 Tg yr⁻¹ of Cl per year in bold):

Photolysis (Sander et al., 2011):

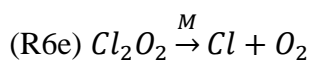
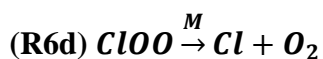
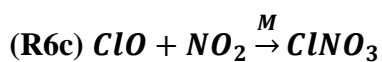
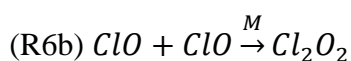
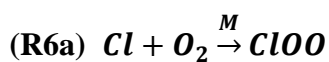




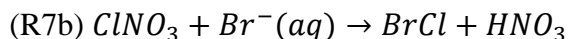
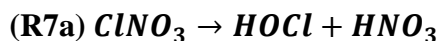
Bimolecular (Sander et al., 2011):



Three body reactions (Sander et al., 2011):



Multiphase reactions



Much of this chemistry is well known due to extensive previous work on understanding the chemistry of the stratosphere.

1.3 VOC oxidation

Ultimately reactive chlorine species are removed from the troposphere through deposition. The most water soluble inorganic chlorine species is HCl. HCl is produced predominantly through the reaction of atomic chlorine with VOCs.

The relative rate constants for oxidation of differing classes of VOCs by OH and Cl varies significantly with carbon number (Figure 1.2). In general reaction with Cl is faster than reaction with OH. This is especially true for alkanes where some species (notably ethane) react significantly (228) faster with Cl than with OH. However, this ratio is not consistent they do not increase linearly or at the same rate. Oxygenated VOCs do not have the same large difference as with alkanes with methanol having the largest difference at 61:1. As the OH concentration is of the order of 10^6 cm^{-3} (Lawrence 2001) and Cl concentrations are predicted to be 1 to 3 orders of magnitude lower (Wingent 1999, Keene et al., 2007), Cl may offer a significant alternative oxidation mechanism for some species.

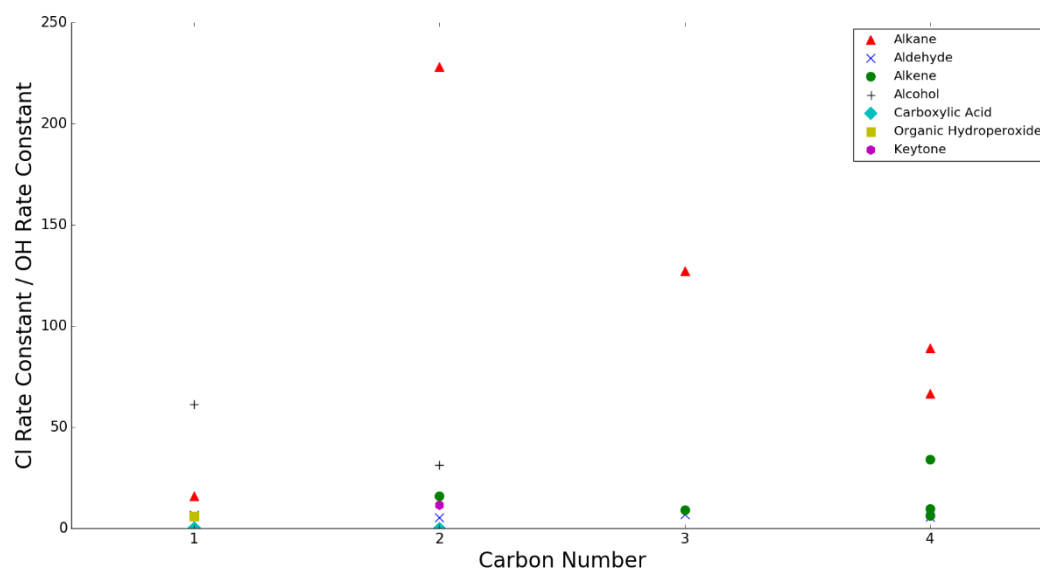


Figure 1.2 shows, for a range of hydrocarbons, their rate constant for reaction with Cl divided by their rate constant for reaction with OH (at STP) (IUPAC).

Some investigations have focused on the effect of Cl on CH₄ oxidation (Lary 2004), however with Cl having a rate constant 15 times that of OH with respect to CH₄ results in atomic Cl only contributing between ~1% (Sherwen et al., 2016) and ~2.5 (Hussain et al., 2016) to total methane oxidation. Given the uncertainty in methane's lifetime to OH (~10% Voulgarakis et al., 2013) it seems unlikely that Cl plays a significant role in the oxidation of methane. However, it may play a more important role determining the isotopic fractionation of methane in some regions (Saueressig et al. 2004).

1.5 Aim of this study

The role of chlorine (and the other halogens) in the troposphere has been discussed over the last 3 decades (Finlayson-Pitts et al., 1989). However, neither measurement techniques nor modelling approaches have been sufficiently developed to be able to offer a methodology to assess its role. Over the last decade though this has changed. Observational approaches (notably for ClNO₂) have allowed new chlorine species to be measured and so new constraints put on this source. However, global models of atmospheric composition are now able to simulate (to some extent) the distribution of chlorine species around the world.

Ordonez et al., 2012 implemented an iodine, bromine, chlorine chemistry scheme into the GEOS-Chem model and discussed the impact of iodine and bromine chemistry on the composition of the troposphere. Although, this model contains significant chlorine chemistry the authors surprisingly make no reference to the concentrations calculated or the impact that this has. A bromine, chlorine scheme was implemented into the GEOS-Chem model by Schmidt et al., 2016 but again here little discussion was made of the impact of chlorine on the composition of the atmosphere. It was not until a Sherwen et al., 2016a that the impact of chlorine chemistry from a global model was first described. However, this description was rather short as the focus of this paper was the combination of the Schmidt et al., 2016 (Br, Cl) work with the Sherwen et al., 2016b (Br, I) to give a coupled I, Br, Cl simulation rather than an emphasis on Cl's atmospheric implication alone. Since the publication of Sherwen et al., 2016, Hussaini et al., 2016 has shown similar results and conclusions within the TOMCAT modelling framework.

The objective of this study is to significantly extend the analysis of the chlorine chemistry simulation in the GEOS-Chem model described briefly by Sherwen et al., 2016. It will provide more extensive insights into the distribution of the different

reactive chlorine species, the processes controlling their distribution, and their impact on atmospheric oxidation. Finally, it will investigate the change in chlorine distribution over the last 20 years, a period when photo-pollutant emissions have moved from the northern hemisphere extra-tropics to the tropics (Zhang et al., 2016).

2. Model Description

The GEOS-Chem global chemical transport model version 10 (<http://www.geos-chem.org>) run at $4^\circ \times 5^\circ$ spatial resolution with 47 vertical levels was used for this study. GEOS-Chem is an extensively used, open-source, atmospheric chemistry transport model which can be run in a variety of global (Bey et al., 2001) and regional configurations (Wang et al., 2004). The meteorological and surface fields (GEOS-5 in this instance) are provided by NASA's Global Modelling and Assimilation Office (GMAO). The model contains the standard O_x , HO_x , NO_x and VOC chemistry (Mao et al., 2013) with the addition of Cl, Br and I chemistry described by Sherwen et al., (2016).

The model used here is the same as that described by Sherwen et al., (2016) but with differences made to the emissions. Rather than describe the model extensively the reader is pointed towards Sherwen et al., 2016. However, the necessity to run the model to investigate changes in chlorine chemistry (1988-2008) over the recent past have led to changes in the emissions used compared to those described in Sherwen et al., (2016) and so they are described in more detail here.

2.1 Anthropogenic emissions

For standard GEOS-Chem configuration, emissions of anthropogenic pollutants (NO , CO , SO_2 , SO_4 and NH_3) come from the EDGAR global inventories (<http://edgar.jrc.ec.europa.eu>), with regional emissions (EMEP, NAI, MIX) databases replacing global where available. However, these regional databases do not extend over the period necessary of this study (1988 and 2008 (Chapter 7)) so for here, the EDGAR emissions are used as they are globally. The seasonal, and diurnal variability of EDGAR emissions are dealt with by the Harvard-NASA emissions component (HEMCO) methodology (Keller et al., 2014) see Table 2.1.

EDGAR provide an emission of a single lumped VOCs. This needs to be allocated to the different primary VOCs considered in GEOS-Chem (ethane, propane, formaldehyde, acetone, PRPE (amalgamated C3+ alkenes), ALK4 (amalgamated C4+ alkanes). The EDGAR VOCs though are provided by sector (transport, solvents etc). Thus, speciation of the EDGAR NMVOC emissions follows that used by the European EMEP regional database at a sector level. The EDGAR emissions sectors are matched to their nearest equivalent EMEP emissions sectors (Table 2.2). A significant downside to this approach is that the EMEP speciation are calculated

based on UK emissions and speciation may well vary regionally rather significantly. There is also some slight variation between what constitutes each EMEP sector relative to its equivalent EDGAR sector.

Table 2.1 How EDGAR emission used in the simulation are handled by the Harvard-NASA emissions component (HEMCO)

Species	Time Step	Seasonal Scale Factor	Diurnal Scale Factor	Speciation Scaling	Notes
NO	Yearly	X	X		
CO	Yearly		X		
SO ₂	Yearly	X			
SO ₄	Yearly	X			Scaled from SO ₂ emissions
NH ₃	Yearly	X			
VOC	Yearly		X	X	

Table 2.2 EMEP sector assigned to each EDGAR sector for speciation.

EDGAR Sector	EMEP Sector
Energy industry	Combustion in energy and transformation industries
Energy for buildings	Non-industrial combustion plants
Combustion in manufacturing industry	Combustion in manufacturing industry
Non-metallic mineral products industry	Production processes
Transformation fossil fuel production refineries steel	Extraction and distribution of fossil fuels and geothermal energy
Solvents	Solvents and other product use
Road transportation	Road transport
Non-road transportation	Other mobile sources and machinery
Solid waste disposal	Waste treatment and disposal

2.2 Halogen and sea-salt aerosol emissions

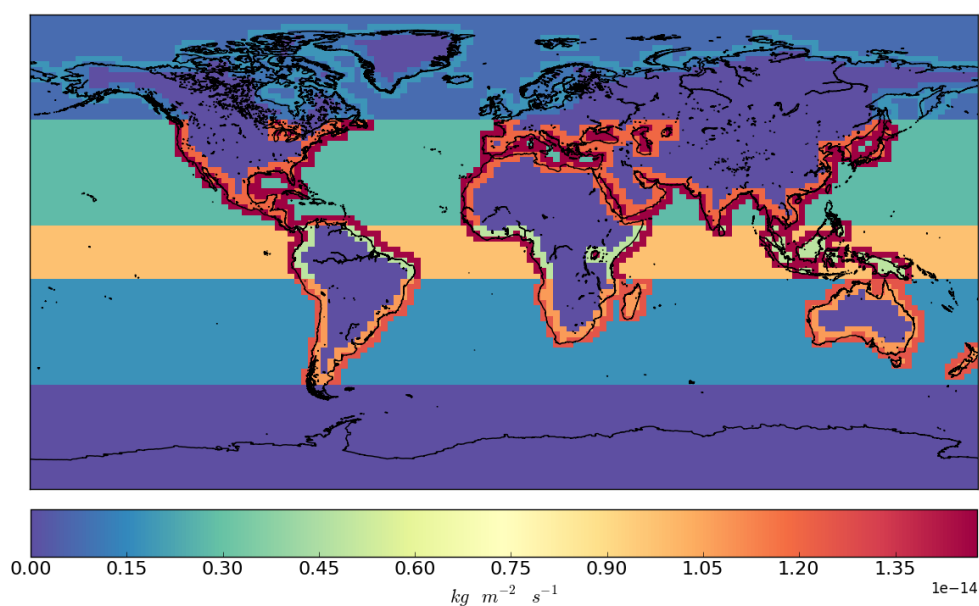
Sea salt aerosol emissions are based on grid box wind speed and sea surface

temperature following Jaeglé et al., (2011) with sea-salt aerosol being distributed between two modes, one fine (0.1-0.5mm) and one coarse (0.5-10 mm)

Short lived organic halogens species CH_3I , CH_2I_2 , CH_2Br_2 and CHBr_3 are emitted into the model based on spatially varying emissions datasets (Ordóñez et al., 2012, Liang et al., 2010) with the methods described in Table 2.3. The remaining longer lived organic halogens (CH_3Br , CH_3Cl , CH_2Cl_2 and CHCl_3) are have fixed surface layer concentration with CH_3Cl , CH_2Cl_2 and CHCl_3 being fixed at 550, 20 and 7 ppt respectively as described by Schmidt et al., 2016. Inorganic emissions of HOI and I_2 are based on O_3 uptake onto the ocean followed by reaction with I^- (Carpenter et al., 2013).

Table 2.3 How the halogen emissions used in the simulation are handled by the Harvard-NASA emissions component (HEMCO)

Species	Time Step	Seasonal Scale Factor
CH_3I	Monthly	
CH_2I_2	Monthly	
CH_2Br_2	Fixed	
CHBr_3	Fixed	X



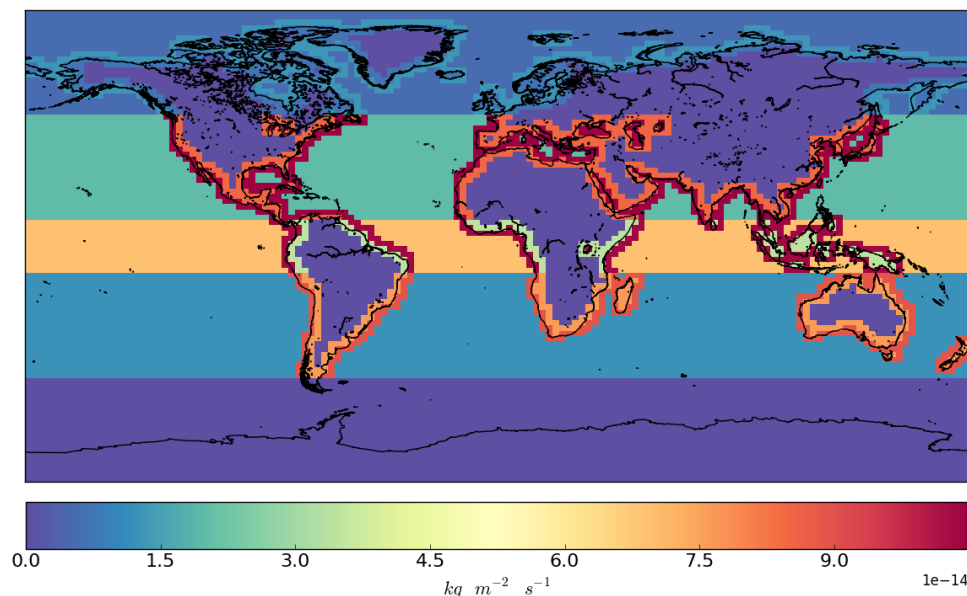


Figure 2.1a (top) 2.1b (bottom). Emissions of CH_2Br_2 (top) and CHBr_3 (bottom).

2.3 Chlorine chemistry scheme

The chlorine update to the standard model we are using for this study has been developed by (Sherwen et al., 2016) which consists of iodine chemistry described by Sherwen et al., 2016, with a bromine and chlorine scheme developed by Schmidt et al., 2016 and Eastham et al., 2014. Eastham added tropospheric chemical and physical processes into the system via the unified chemistry extension (UCX). Schmidt et al., 2016 updated the tropospheric bromine mechanism originally described by Parrella et al., (2012), to include a more extensive multiphase chemistry mechanism and a simulation of tropospheric chlorine radical chemistry.

Much of the chemistry in the model is described in the introductory chapter. There are many potential limitations of the model chlorine chemistry scheme. The model consists of organochlorine emissions for CH_3Cl , CH_2Cl_2 and CHCl_3 which then assumes a unit release of all Cl atoms in the molecule. However, Hossaini et al., (2016) shows that the deposition of chlorinated compounds which form part of the oxidation chain of these compounds can be significant and lead to a significantly lower conversion factor organic chlorine to reactive chlorine. The model also missed direct anthropogenic sources of inorganic chlorine from coal burning, swimming pools, salt lakes etc which may explain some observations of high ClNO_2 etc in continental regions (Thornton et al, 2010). The model also only represents chloride in the fine and coarse sea-salt aerosol modes. Thus, there is no chloride in the very fine sulfate mode. One potential explanation for the continental chloride observations is

the release of reactive chlorine from the sea-salt which then becomes HCl and can be absorbed into sulfate aerosol which it can be transported long distances (Thornton et al., 2010).

Sherwen et al., (2016) describes some limited comparison between observations and model for Cl species. Notable is the model's inability to reproduce continental ClNO₂ concentrations, likely due to the reasons outlined above. As such, the model probably provides for a lower limit for the tropospheric at reactive Cl

2.4 Transportation and deposition

Transport between grid boxes occurs in 30 minute time steps and is calculated from the 3D wind fields, convective mass fluxes and vertical diffusion constants (K_{zz}) provided from the meteorological data. The transport configuration of GEOS-Chem is well described by Wu et al., 2007.

Deposition to the surface offers the end step for many atmospheric chemistry processes. GEOS-Chem describes this processes in term both wet and dry processes. Wet process involve clouds and id described in terms of washout, rainout and scavenging in convection updrafts (Wu et al., 2007). Dry process deposition is based on the "Wesley" resistance-in-series scheme implemented by Wang et al. (1998).

2.5 Simulations performed

In this study, the code of described in Sherwen et al., 2016 is used with the changes to the anthropogenic emissions described above. We define the "present day" as the year 2008, running the simulation from 1st January 2007 to 1st of January 2009. The reason for this year being used as our present-day period is due to this being the most recent year that we have global EDGAR data, beyond this period regional databases take over which will cause inconsistencies. The first year (2007) of data being considered the "spin up" year (preventing any influence from the initial conditions affecting results) and is thus being discarded.

Where a historical (1988) simulation is run, the same (2008) meteorology is used but with changes to the anthropogenic emissions. This allows a much shorter simulation (2 years) to be run to assess significant changes than if simulations with the time specific meteorology was used (~10 years).

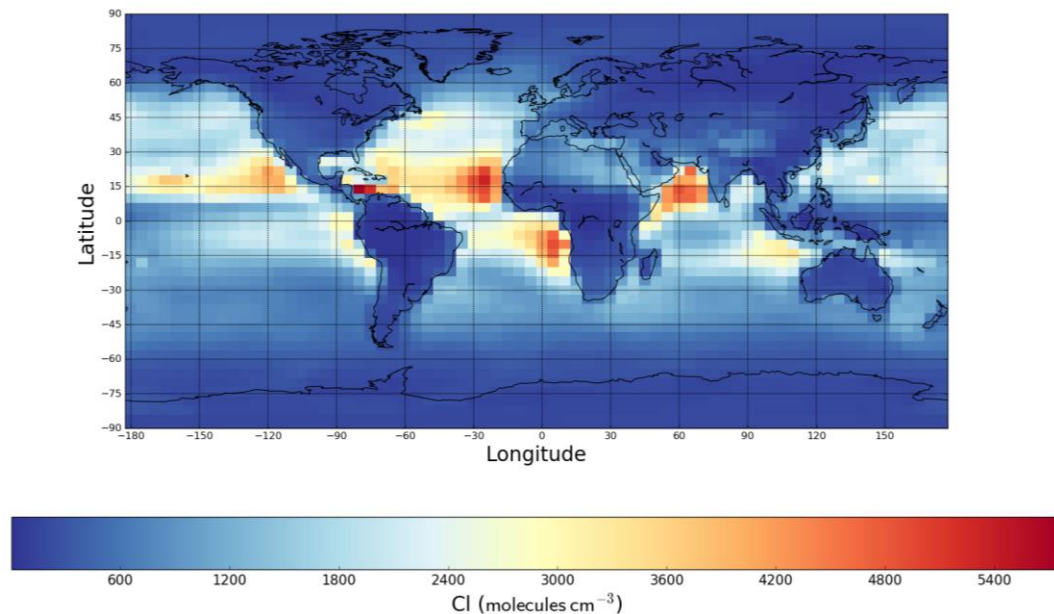
3. Global Distribution of Atomic Chlorine

In this chapter the spatial and temporal distribution of atomic chlorine calculated by the model for the present day (nominally 2008) is discussed. We initially start by discussing the concentrations at sea-level and then within the lowest 500hPa of the atmosphere. We then look at the distribution through the column and in the zonal mean.

3.1 Sea level chlorine

At sea level the mean Cl concentration for 2008 is $1083 \text{ Cl atoms cm}^3$, with highs of $1 - 5.5 \times 10^4$ the same found by Hossaini et al., (2016)

At sea level, atomic Cl is located mainly in the sub tropics almost exclusively over marine region (Figure 3.1a). Cl has a northern hemisphere bias, with 57.5% located in the Northern Hemisphere seen in figure 3.1b. The sea level atomic Cl is regionally specific, with regions such as the north Indian ocean and the west African coast experiencing concentrations approximately twice that of other areas of similar latitude.



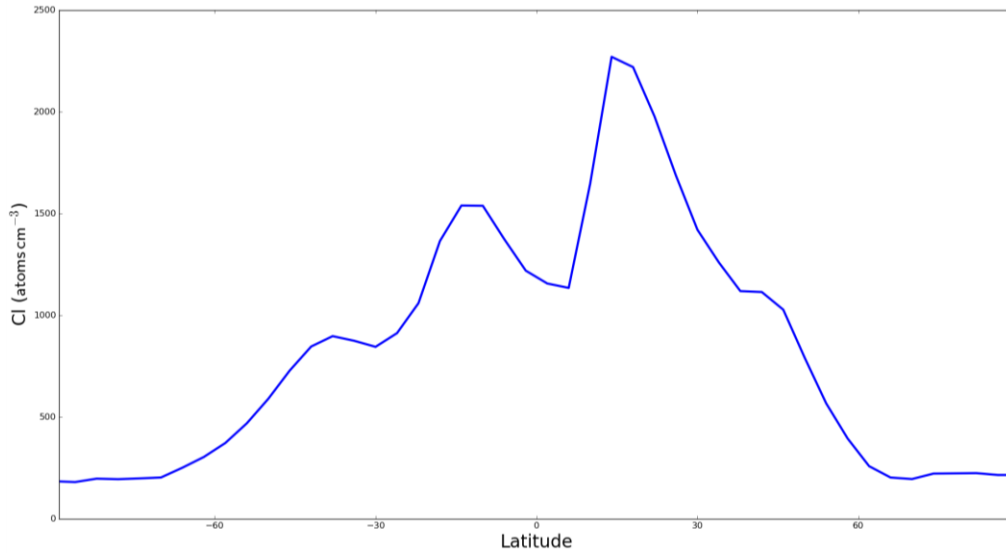
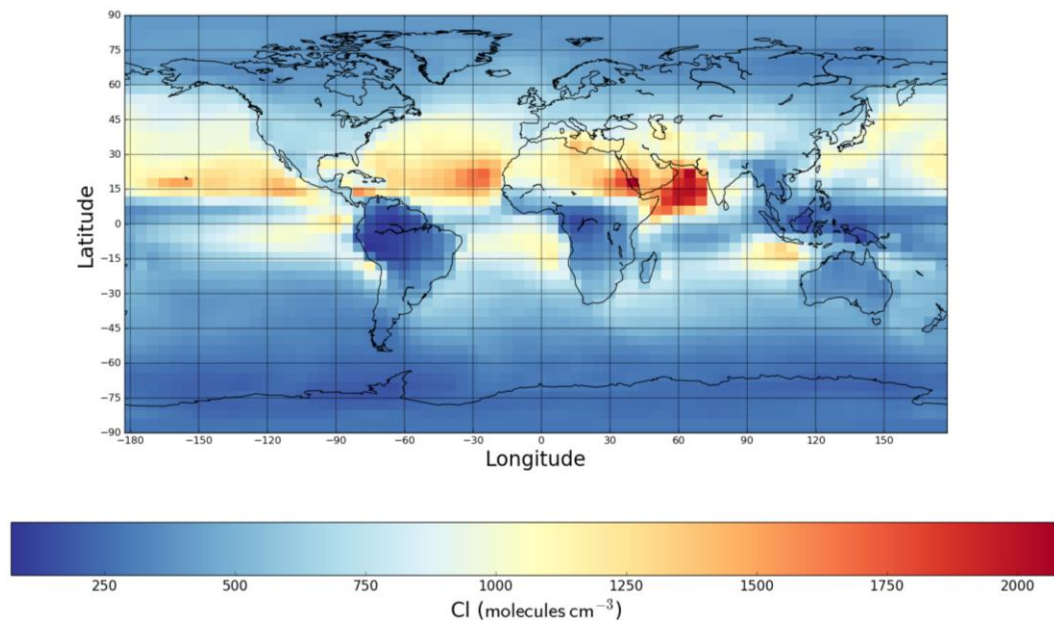


Figure 3.1a (top) 3.1b (bottom). 3.1a shows Cl concentration averaged over 2008 in molecules cm⁻² from ground level to 589m altitude (the first 5 levels of GEOS-Chem). 3.1b shows Cl atoms integrated across each latitude.

3.2 Ground to 500 hPa

On average between the surface and 500 hPa the mean atomic Cl concentration is 644 Cl atoms cm⁻³ lower than that at the surface. The spatial distribution shows similar patterns as the atomic chlorine at the surface. The delineation between marine and non-marine areas becomes less strong with high atomic Cl concentrations found over the Africa desert regions (Figure 3.2a). The northern hemisphere dominance of Cl increases (Figure 3.2) with 62% of the total atomic chlorine being found in the North Hemisphere.



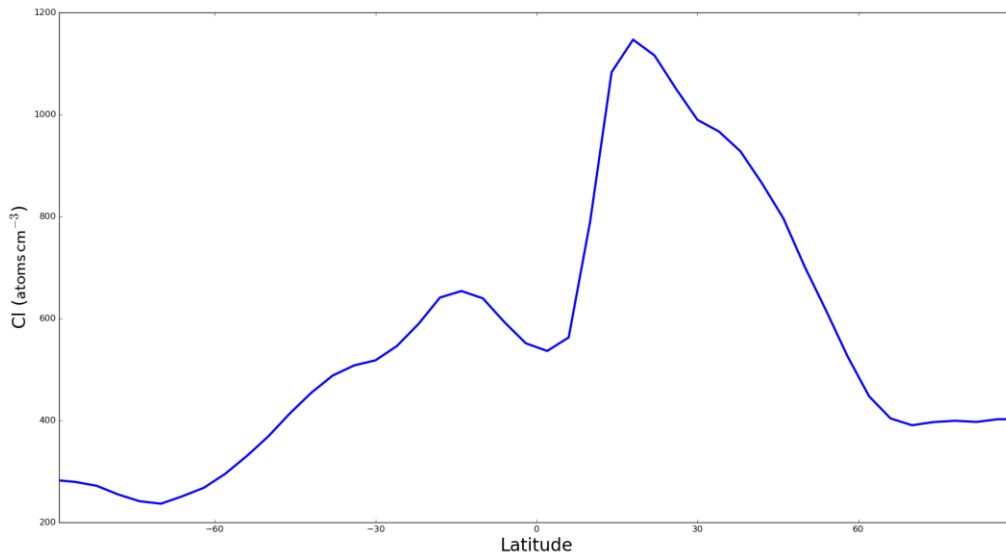


Figure 3.2a (top) 3.2b (bottom). 3.2a shows Cl concentration averaged over 2008 in Cl atoms cm⁻² from ground level to the 500 hPa pressure level (the first 23 levels of GEOS-Chem). 3.2b shows Cl atoms averaged across each latitude.

3.3 Ground to tropopause

Throughout the whole column the average atomic Cl concentration is 495 Cl atoms cm³, less than have the mean value of 1.3×10^3 cm⁻³ found by Hossaini (2016). The atomic Cl is concentrated heavily in the northern hemisphere between 0° and 45° latitude with the highest concentrations over marine regions (Figure 3.3a), although with much higher levels of atomic Cl over land than seen at the other two column heights. 60.5% of global tropospheric Cl is located in the northern hemisphere (Figure 3.3b). As with the northern hemisphere the southern hemisphere also shows predominance in the subtropical and temperate regions. In the zonal plot (Figure 3.3c), it can be seen that the highest concentrations of atomic Cl are present (> 2000 Cl cm⁻³) are at low altitude (< 1000 m) in the northern tropical and subtropical regions.

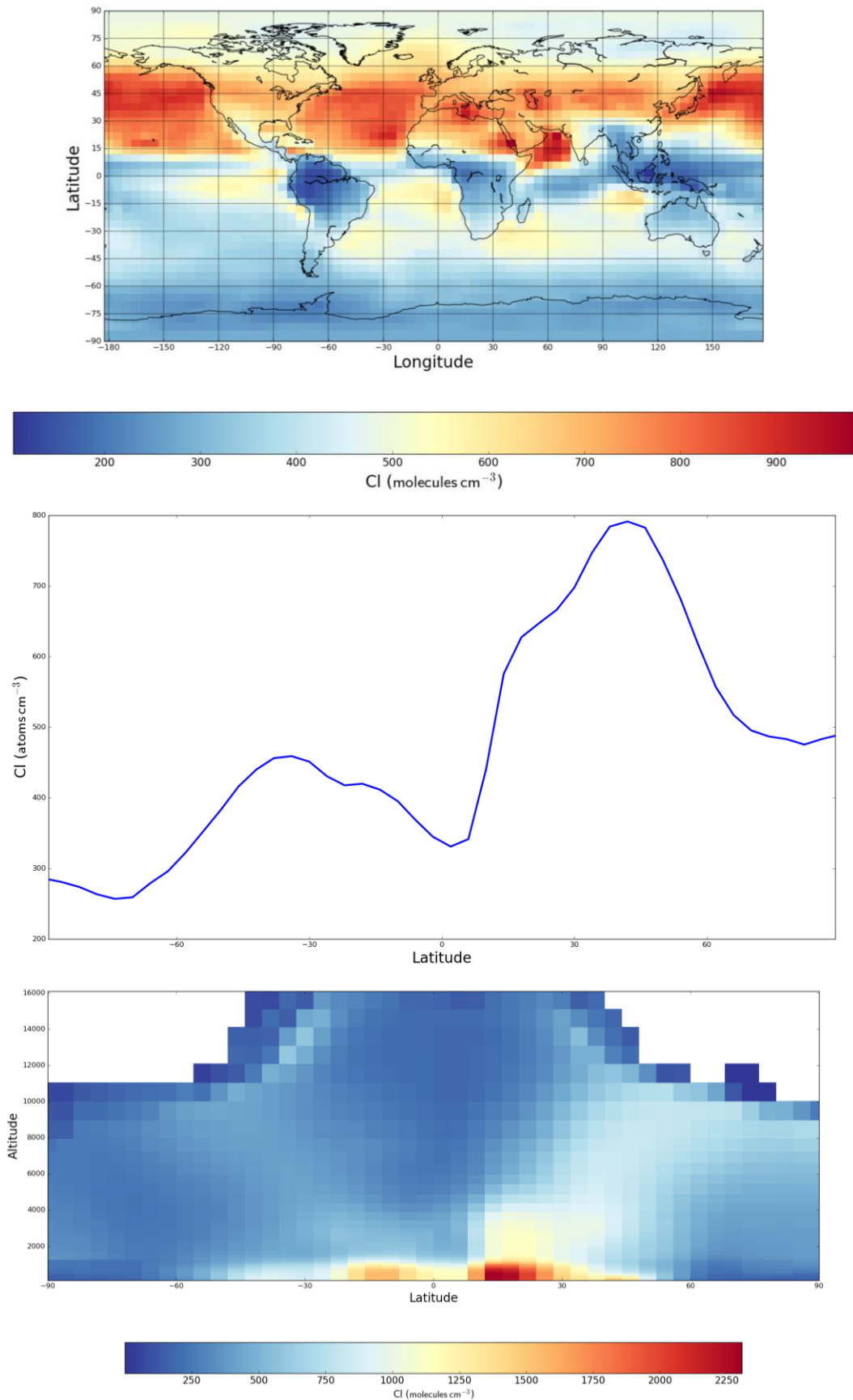


Figure 3.3a (top), 3.3b (middle) and 3.3c (bottom). 3.3a is the Cl concentration averaged over 2008 in Cl atoms cm^{-2} from ground level to tropopause, 3.3b is the Cl

atoms averaged across each latitude. 3.3c is a zonal plot of Cl masked beyond the tropopause in Cl atoms cm⁻².

3.4 Summary

For the present day the mass weighted mean atomic Cl concentration is 495 cm⁻³.

This compares to 1.3×10^3 cm⁻³ modelled recently by Hossaini (2016)

We find that the highest concentrations are located with the marine boundary layer in tropical regions with a preference towards the north hemisphere. With levels of $1 - 5.5 \times 10^4$ cm⁻³ the same values found by Hossaini et al., (2016)

In the next chapter the sources of atomic chlorine in the model are discussed.

4. Atomic Chlorine Sources

As discussed in the introduction there are a range of routes to produce atomic chlorine in the model. In this section, we examine the sources of atomic chlorine (Section 4.1) and then examine the sources of these source species. (Section 4.2-4.5).

4.1 Cl production routes

At sea level, photolysis of BrCl produces the vast majority of Cl with 78% of production coming via this route. ICl photolysis, chloromethane reacting with OH produces, ClNO₂ photolysis and HCl reacting with OH contributing 9, 6.7, 5.5 and 1 respectively.

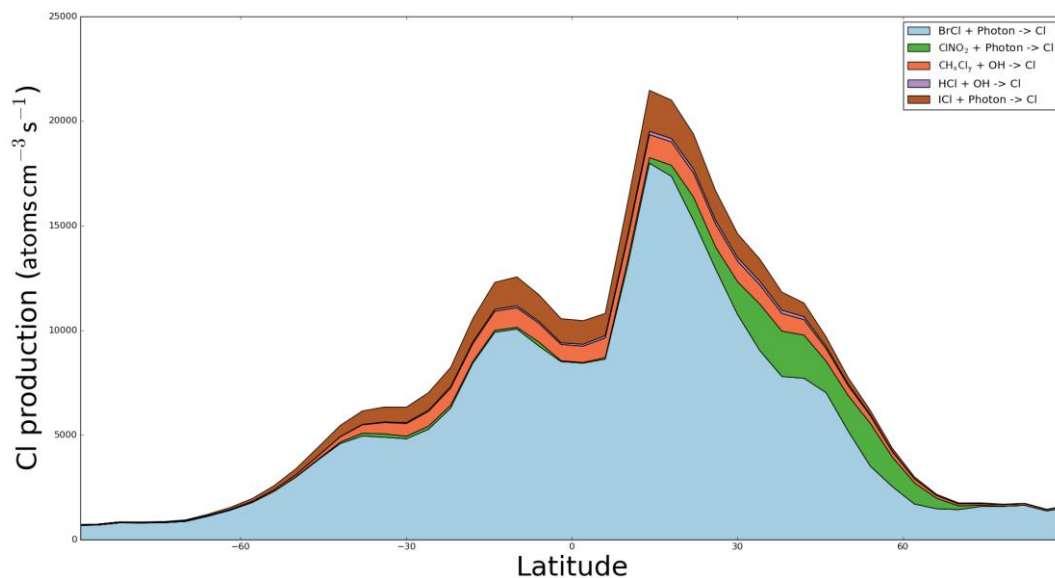


Figure 4.1 shows the zonal sea-level production of atomic Cl.

When considered for the whole tropospheric column the story remains the same. Photolysis of BrCl still dominates production (77%), but with an increased importance for the organic sources of chlorine from OH reaction (11.75%). The importance of HCl reacting OH becomes increases (5.75%) but the ICl and ClNO₂ photolysis become much less important (3.5% and 2% respectively).

Thus over the whole column photolysis of BrCl is the dominant source of atomic chlorine. However, the importance of minor channels changes between essentially sources which have a surface (notably short lived sea-salt) component (ICl, ClNO₂) and those which have a longer lived sources (organic chlorine species and HCl). This can be seen clearly in Figure 4.3. It is also clear the atomic Cl production is largest in the boundary layer and drops off with altitude.

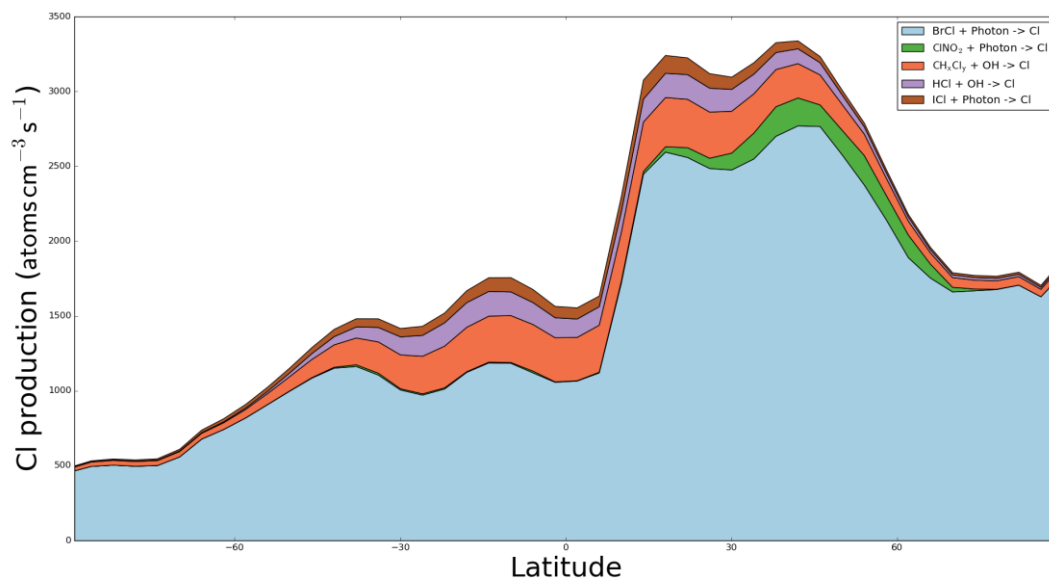


Figure 4.2 Average 2008 production of Cl atoms intergraded over the whole column averaged across each latitude.

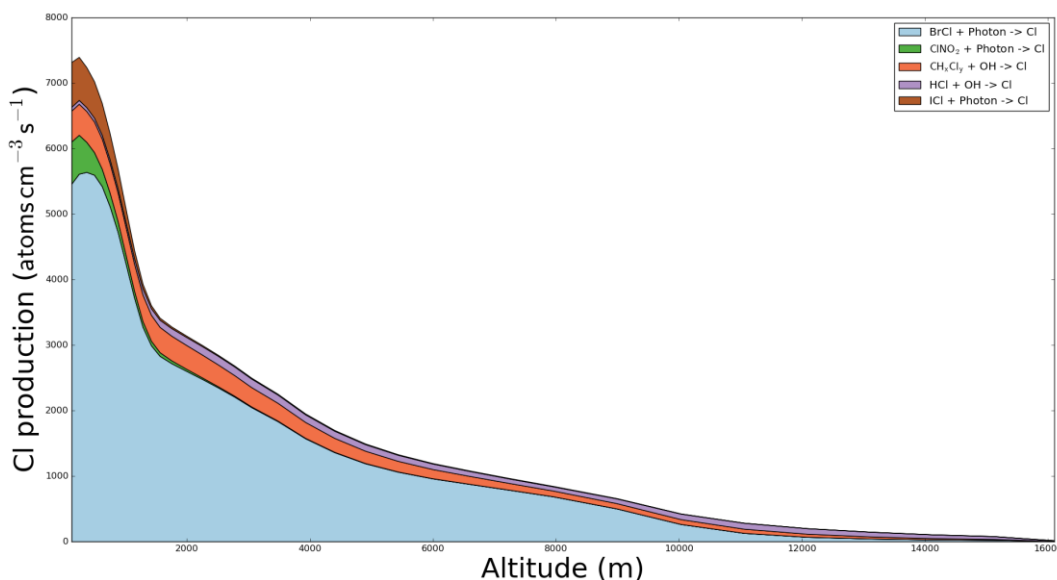
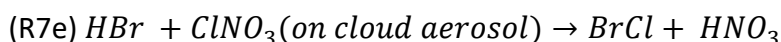
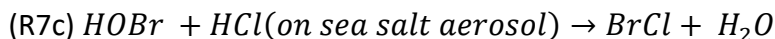
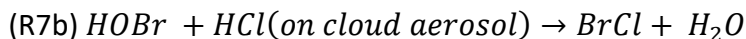
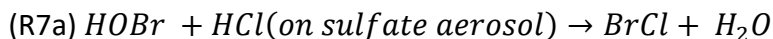


Figure 4.3 Average 2008 production of Cl atoms $\text{cm}^{-3} \text{s}^{-1}$ averaged for each vertical level.

From this analysis, it is obvious that to understand the distribution of Cl described in Chapter 3 it is necessary to understand the sources of its precursors. Thus in section 4.2 we investigate the sources of BrCl, section 4.3 ClNO₂, section 4.4 decomposition of organic chlorine compounds and ICl section 4.5.

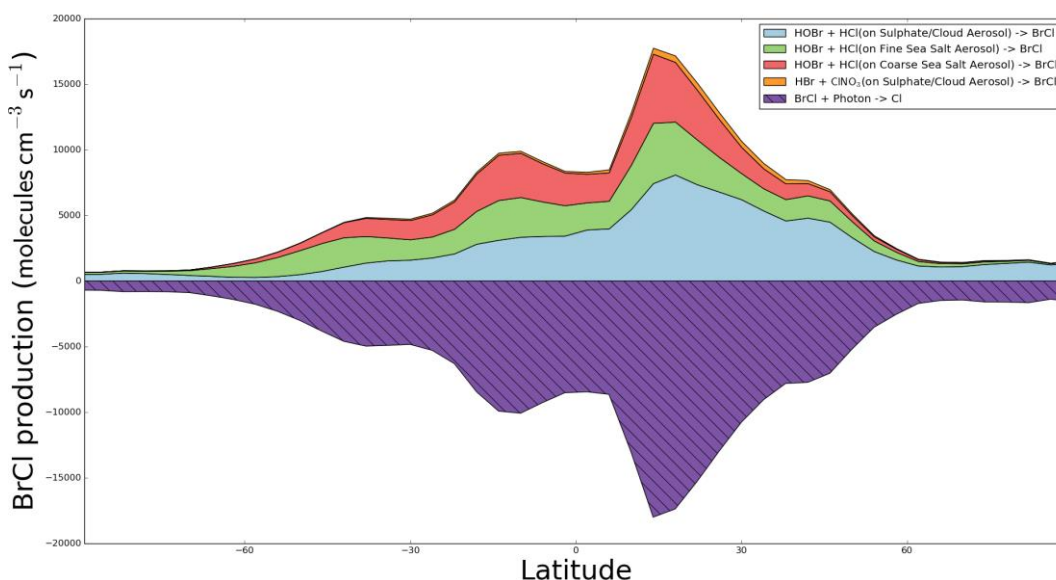
4.2 BrCl

Within the model BrCl has a tropospheric lifetime of approximately 1 hour. It is made through a number of heterogeneous reactions in the model (R7a-e) and its sole sink in the model is photolysis into atomic Br and Cl:



Within the chlorine representation of GEOS-Chem, R1a and R1b are combined, and R1c is broken down into reaction on fine sea salt and coarse sea salt. Reactions R1d and e only produces 2 - 3% of BrCl.

At sea level (Figure 4.4a), reaction of HOBr and HCl on sea salt aerosol is the dominant source of BrCl making up 53% of BrCl production. Reaction of HOBr on sulphate aerosol and cloud droplet makes up 44.5% with the remaining 2.5% coming from the ClNO₃ cycling reaction. The sea-salt aerosol source has a similar flux in both hemispheres, however, the reaction due to sulphate/cloud aerosol produces $3.1 \times 10^8 \text{ BrCl cm}^{-2} \text{ s}^{-1}$ in the northern hemisphere compared to $1.2 \times 10^8 \text{ BrCl cm}^{-2} \text{ s}^{-1}$ in the southern hemisphere. Given that both hemispheres have almost equal cloud cover (Figure 4.4b) this imbalance must be due to the pre-ponderous of sulfate aerosol surface area in the northern hemisphere.



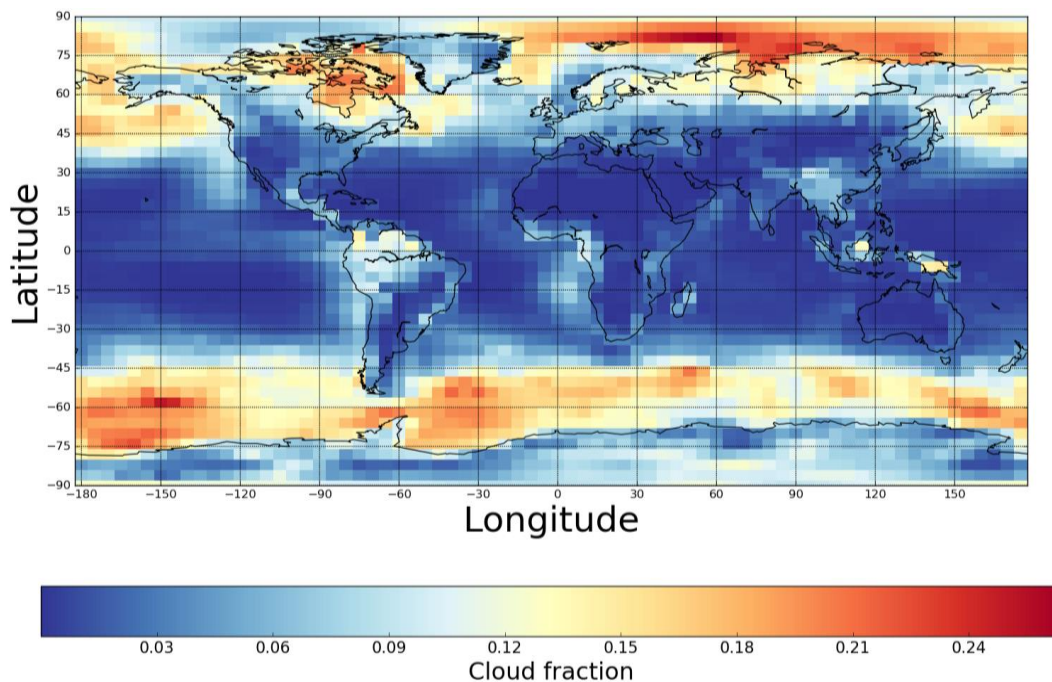


Figure 4.4a (top) and 4.4b (bottom). The average 2008 production of BrCl molecules in molecules $\text{cm}^2 \text{s}^{-1}$ for sea level (4.4a) averaged across each latitude. The average 2008 cloud fraction (4.4b) at sea level.

As at sea level, globally the northern hemisphere source of BrCl is 2.5 times higher than the southern hemisphere. Cloud fractions between the northern and southern hemisphere are split fairly equally (Figure 4.5c), again suggesting that reaction R1a on sulphate aerosol is the dominant route for BrCl production. As R1a produces 75.5% of atmospheric BrCl over the whole column, and BrCl photolysis produces 77% of Cl, reaction R1 is responsible for approximately 58% of global Cl production in the model.

Over the whole column, reaction of HOBr with HCl on sulphate and cloud aerosol (R1a/b) is the dominant (75%) route for BrCl production approximately. Reaction on sea salt contribute 11.5% and 10.5% on fine and coarse salt respectively. As seen in Figure 4.5b these sea salt aerosol reactions drop off rapidly with altitude, producing only a very small proportion of BrCl by 2000 m. The reduction in the sea-salt surface area with altitude is the reason for the steep reduction in Cl production over the lowermost 2000m of the atmosphere (Figure 4.3). As SO_4 distribution is largely a result of anthropogenic activity this alludes to the largest route to Cl production globally having a strong human influence and explains the northern hemisphere dominance witnessed in Cl concentration.

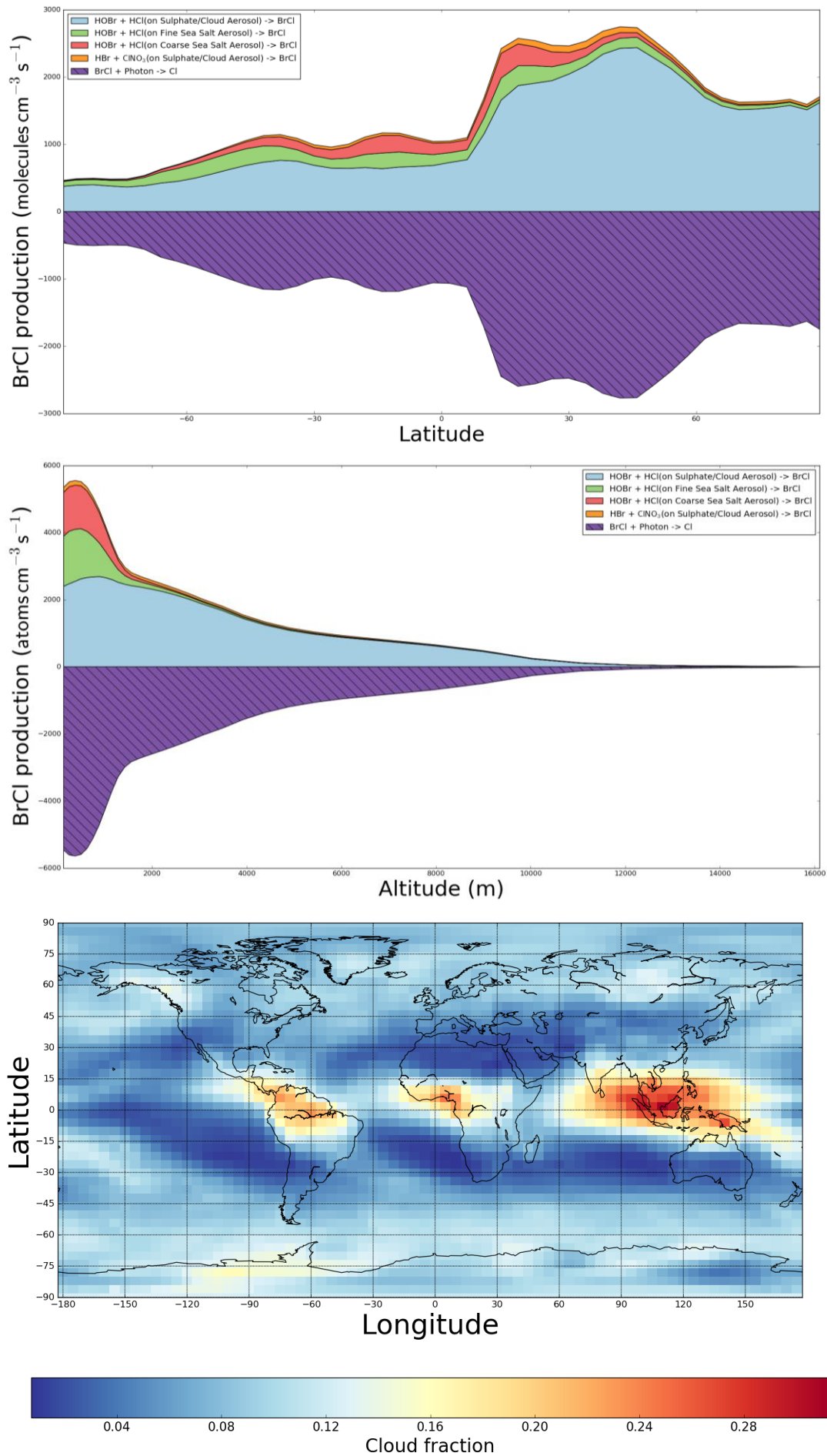


Figure 4.5a (top) ,4.5b (middle) and 4.5c (bottom) The average 2008 production

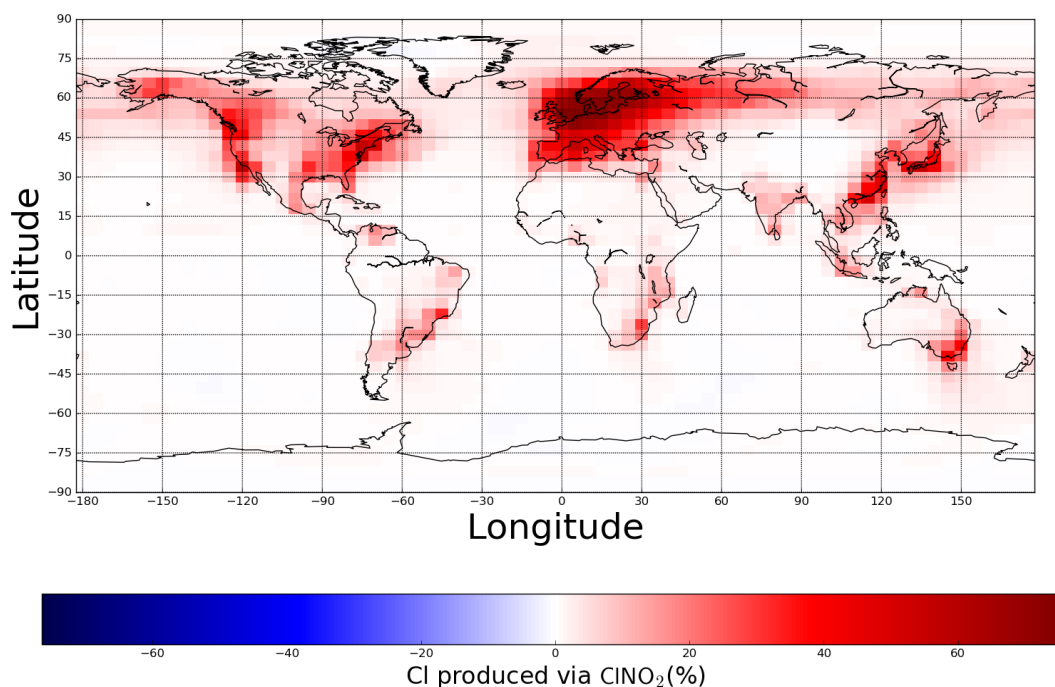
of BrCl molecules in molecules $\text{cm}^2 \text{s}^{-1}$ for whole column (4.5a) averaged across each latitude. BrCl production averaged over each vertical level of the model (4.5b). The average 2008 cloud fraction (4.5c) at sea level.

A previous study by Walker et al., in 2012 found sulphate predictions in the simulation to be in reasonably good agreement with observation data.

4.3 Sources of ClNO₂

After BrCl photolysis, ClNO₂ photolysis is the next largest anthropogenic atomic Cl source (see Figure 4.1).

ClNO₂ production requires high NO_x concentrations due to the requirement of NO₂ and NO₃ to produce N₂O₅. Coupled with its reliance on sea salt aerosol, ClNO₂ is only really important over polluted coastal regions. In Figure 4.8 the model was run without ClNO₂ production from the N₂O₅ reaction on sea-salt. At sea level over polluted coastal regions ClNO₂ is a very important route to atomic Cl production making up around 50% of production over significant areas. Over Europe it can be responsible for over 60% of Cl. Due to the reactions reliance on sea salt aerosol, the importance ClNO₂ as a Cl source falls with altitude, accounting for 10% of Cl produced over the whole column in Europe (Figure 4.8b).



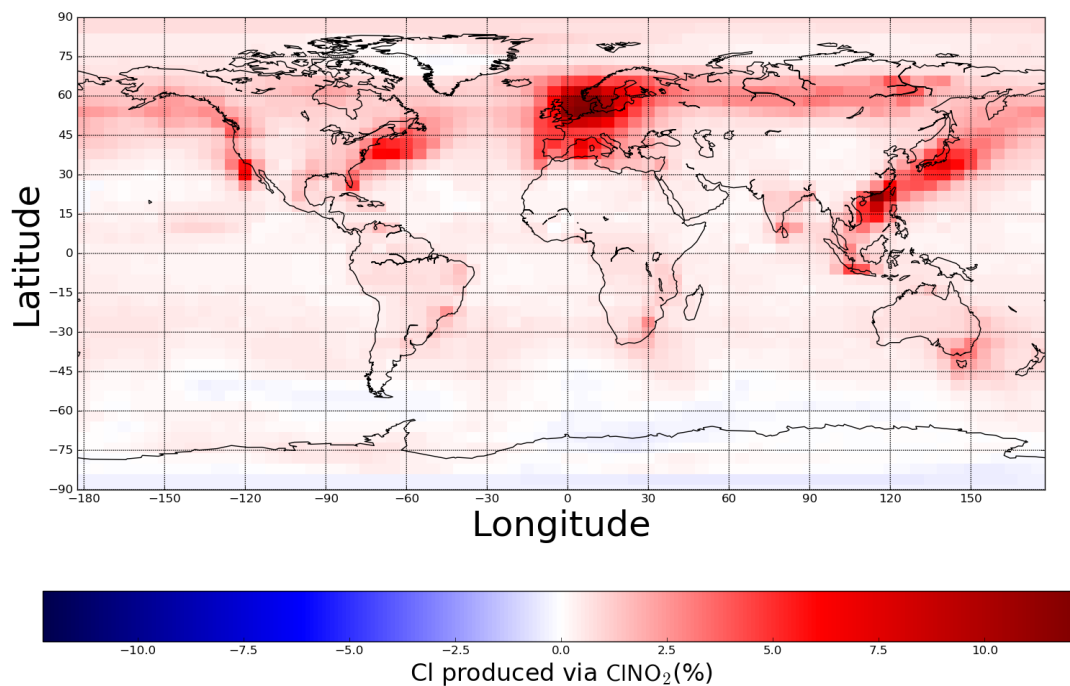


Figure 4.8a (Top) and 4.8b (Bottom). Cl concentration due to the inclusion of ClNO₂ in the simulation, sea level (4.8a) and whole column (4.8b).

Figure 4.9 shows the variation in Cl sources as a function of latitudes for a band over the European longitudes. This shows the profound impact the ClNO₂ photolysis can have on Cl production in regions with high NO_x emissions. Due to the steep drop off in sea-salt with altitude, this route creates a shallow (approximately 1500 m) “bubble” of high Cl air over high NO_x regions. This may play a potentially important role in determining the chemistry of the air in these polluted regions.

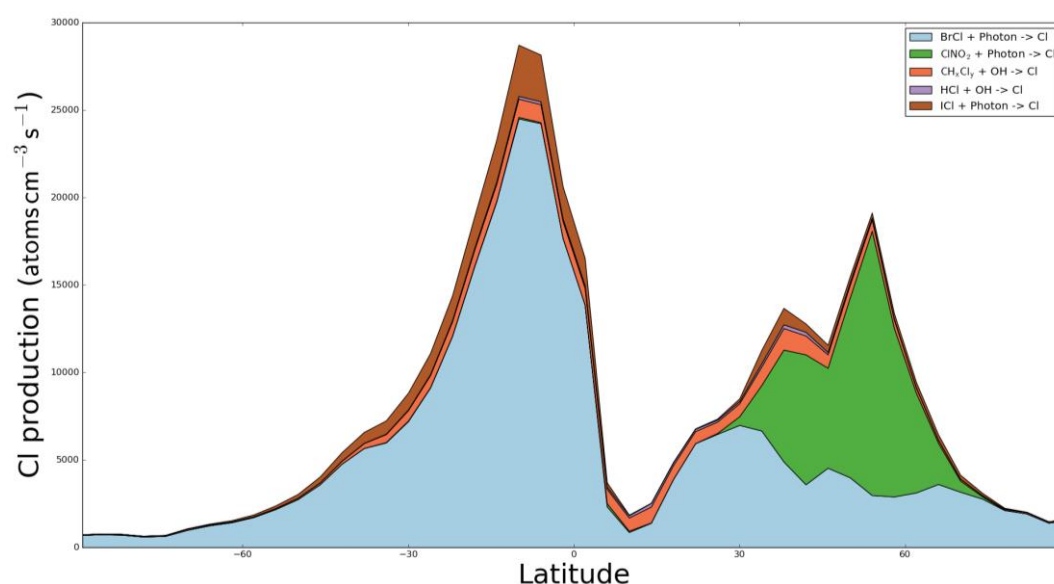


Figure 4.9 Average 2008 production of Cl atoms for sea level averaged across each latitude between -5 and 20 degrees' longitude.

Due to the reliance of this route on NO_x concentration, it can be assumed this production route is sensitive to the changes in NO_x emissions that have happened over the last 20 years and will be investigated in section 7.

A previous study by Wang et al., in 2011 found that NO_2 in the simulation was over predicted by about 8 %, while Lamesal et al., 2015 and Oetjen et al., 2013 found the agreement to be within around 20% of ground based and aircraft observations respectively.

4.4 Sources from the decomposition of organic chlorine compounds

Almost all of the organic chlorine decomposition in the troposphere occurs via reaction with OH. Photolytic sources are small due to the lack of photons of the appropriate wavelength. At sea level (Figure 4.10a) the reaction between OH and these species produces around 6% of the atomic chlorine with that sourced 73.75 %, 17.5% and 8.75 % CH_3Cl , CH_2Cl_2 and CHCl_3 produce of the Cl respectively at sea level (Figure 4.10a). At sea level much of the spatial distribution of this source matches the OH concentration (figure 4.10b). The OH concentration in the northern hemisphere (driven by greater pollution) results in a higher the northern hemisphere source for Cl.

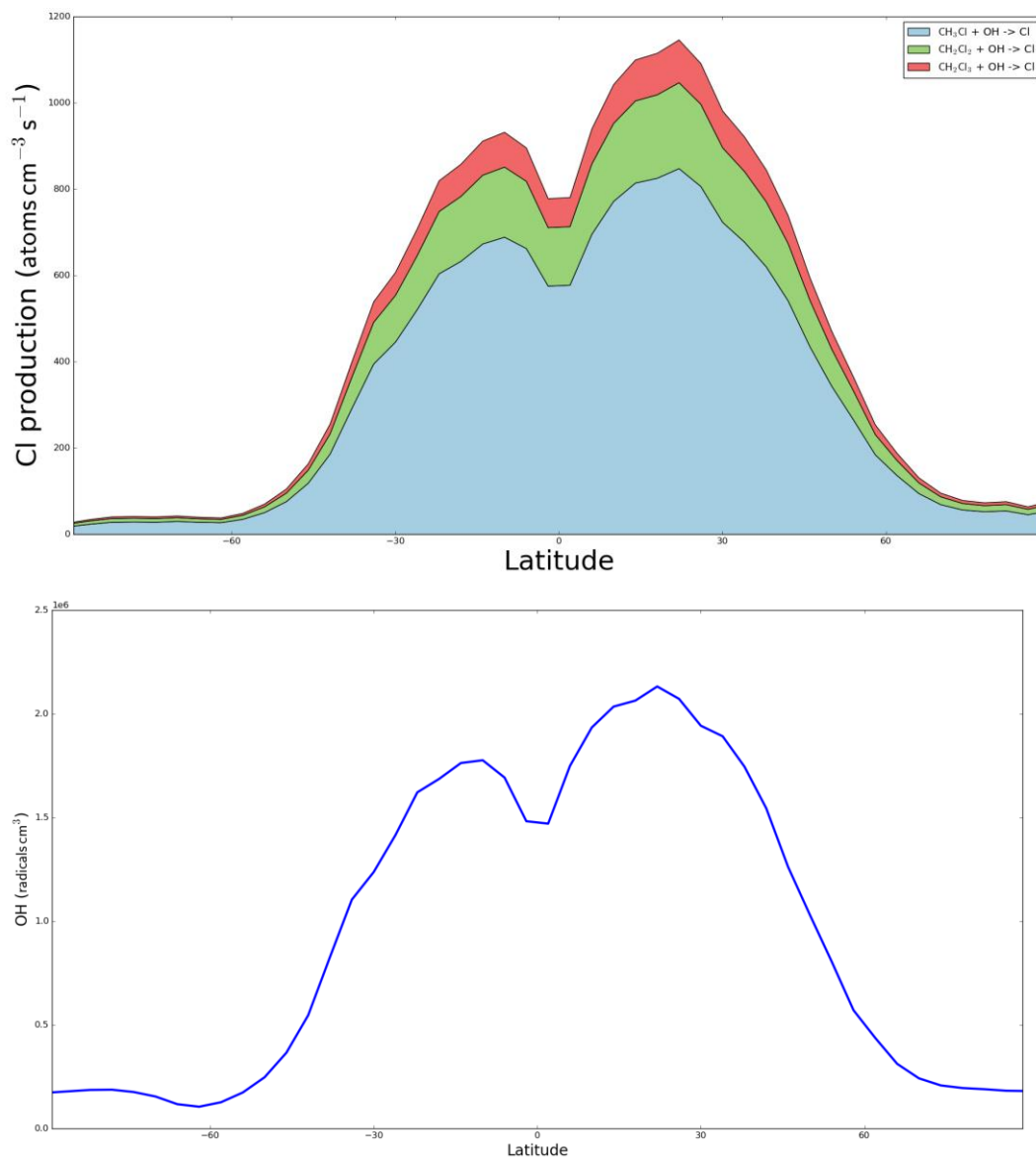


Figure 4.10a (top) and 4.10b (bottom). The average 2008 production of Cl atoms cm⁻² s⁻¹ from organic chlorine (4.10a) and OH concentration (4.10b) at sea level averaged across each latitude.

Globally, decomposition of organic chlorine is the second largest global source of Cl (12%) with the split between the different organic species comparable to that at sea-level (CH₃Cl, CH₂Cl₂ and CHCl₃ producing 73 %, 18.25 % and 8.75 % respectively) (figure 4.11a). Over the whole column OH concentrations are more equal and so production of Cl via this route is close to equal between hemispheres (see Figure 4.11b).

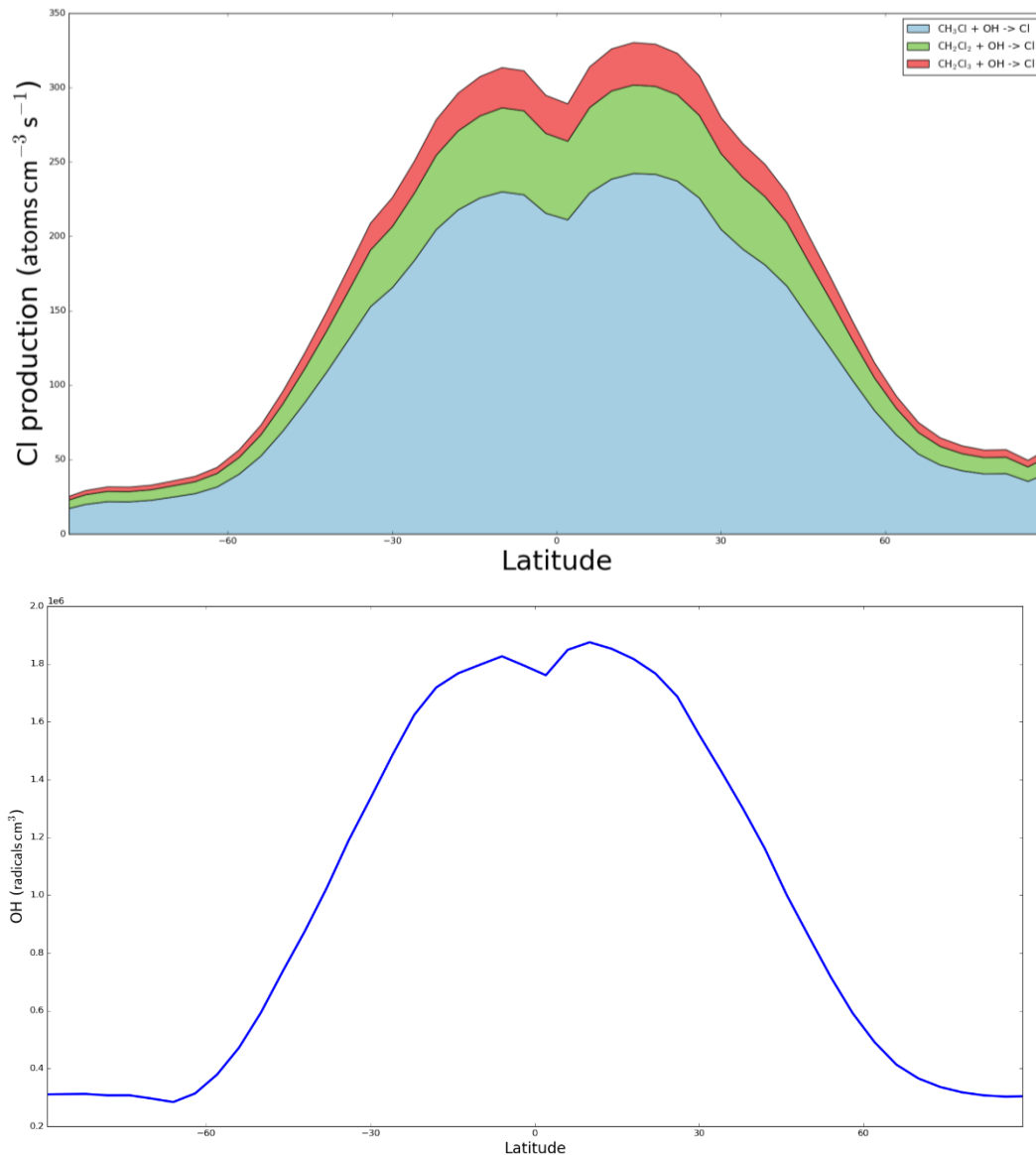


Figure 4.11a (top) and 4.11b(bottom). The average 2008 production of Cl atoms cm⁻² s⁻¹ from organic chlorine (4.11a) and OH concentration (4.11b) for whole column averaged across each latitude.

CH₃Cl and CH₂Cl₂ can also act as a source of Cl through photolysis and reaction with Cl however these routes provide an insignificant source of Cl (less than 0.1% overall).

4.5 Source from ICl photolysis

ICl has multiple sources. There is a small source (15% globally) from the reaction of IO with ClO. This isn't a net source of Cl as it acts to recycle Cl species.

The majority (76%) of this heterogeneous ICl production comes via reaction with HOI (R1a), reaction with IONO₂ contributes the rest (16%) (See Figure 4.12). The IONO reaction (R1c) produces less than 0.1%. As all Cl production routes via ICl

involve sea salt aerosol, these reactions happen solely in marine regions, and so occur only within the marine boundary layer (Figure 4.13c).

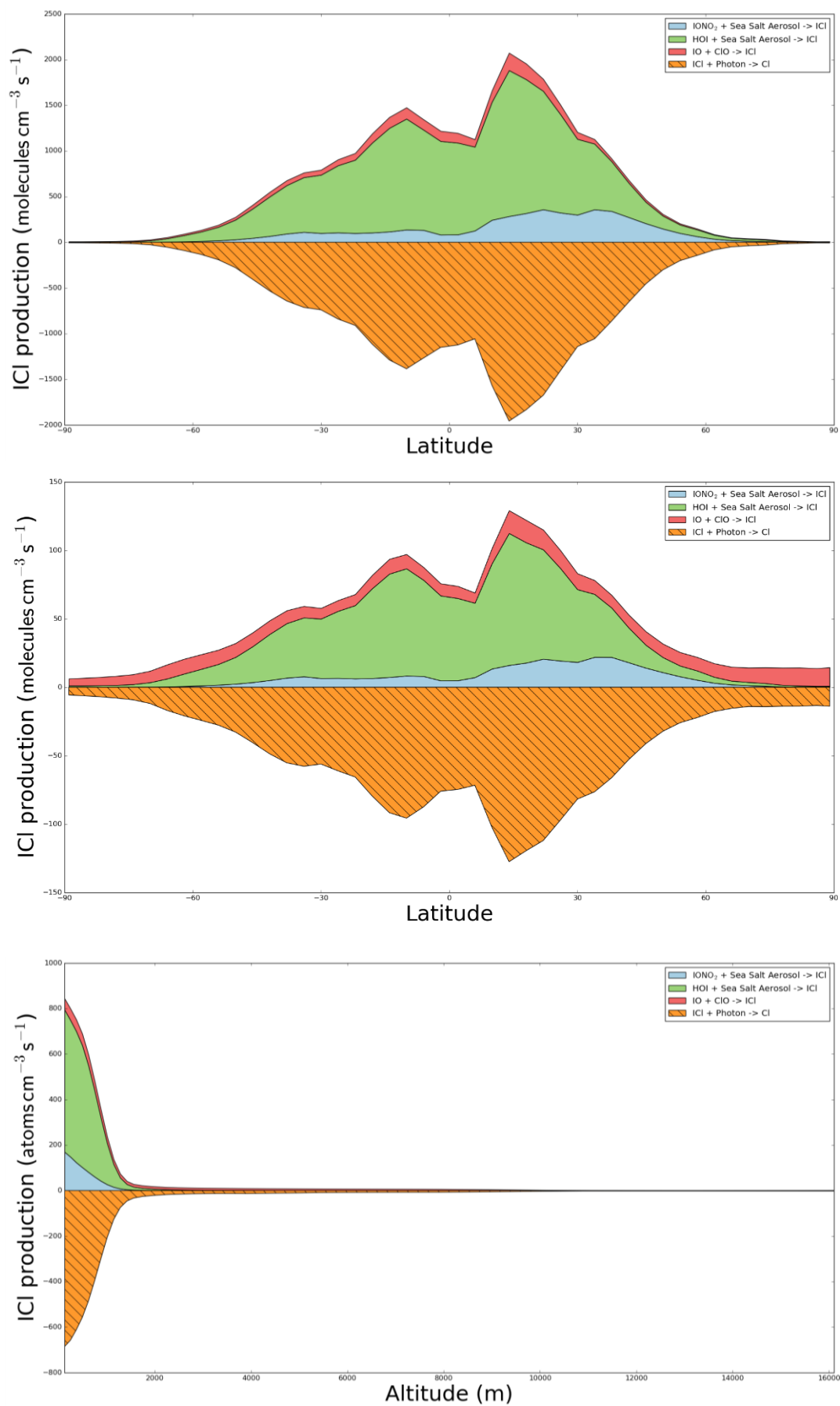


Figure 4.12a (top), 4.12b (middle) and 4.12c (top) The average 2008 production of ICl molecules for sea level (4.12a) and whole column (4.12b) averaged across each latitude. 4.12c is the production of ICl molecules averaged over each vertical level.

4.6 Summary

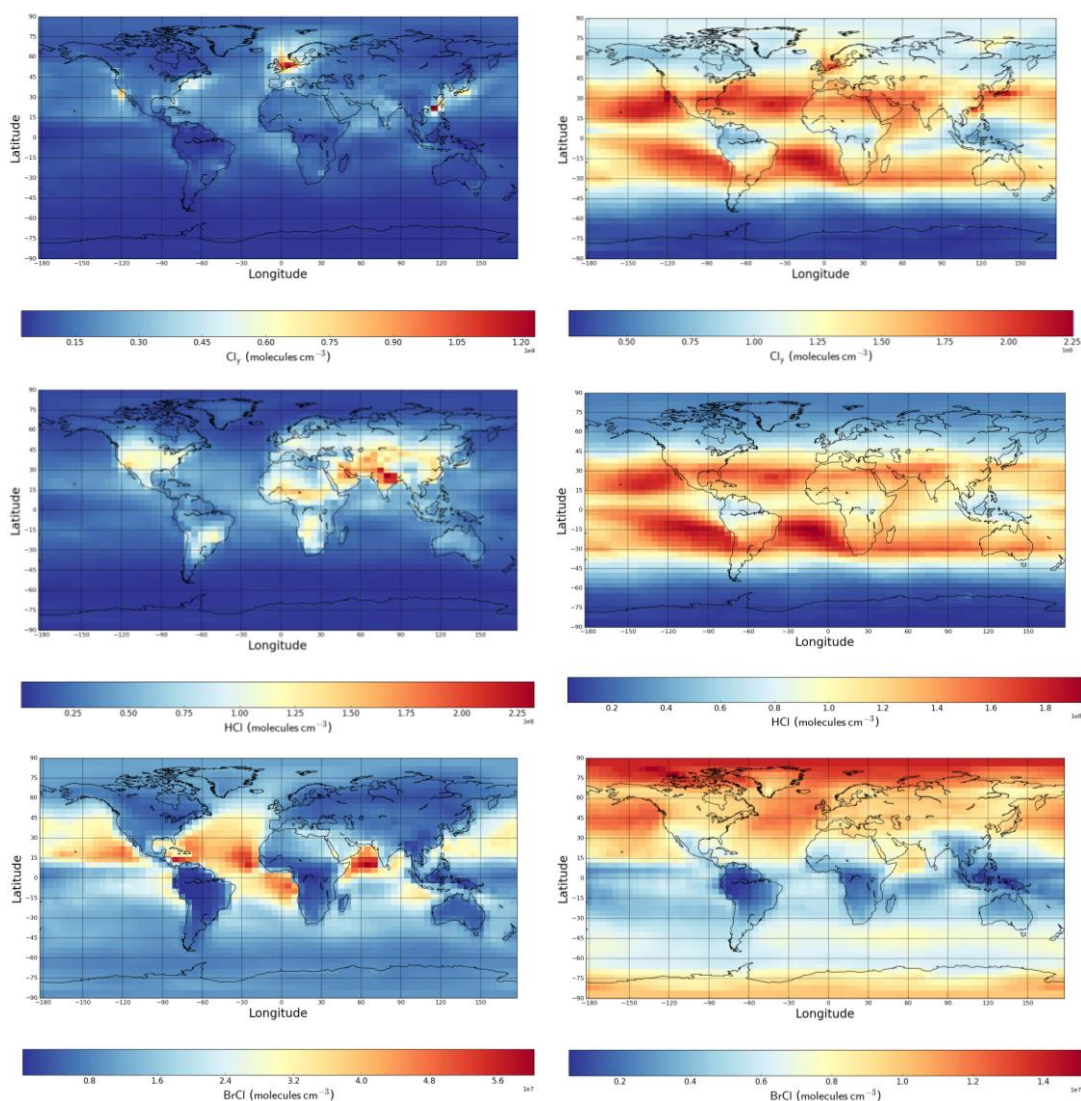
Globally the reaction between HOBr and HCl on sulfate aerosol dominates the production of Cl precursors through its production of BrCl but in the boundary layer sea-salt sources through reaction with N_2O_5 or iodine species can dominate. HCl plays a complex role here. Its role as a direct source of Cl through the reaction of HCl with OH is small however, as parameterized in the model, heterogeneous reactions which convert HCl into more photo-labile species plays an important role.

5. Chlorine Species and Cycling

In the previous chapters the focus has been on the distribution and sources of atomic Cl. In this chapter the concentration of other Cl species calculated by the model is described and then the cycling of chlorine species within the model is investigated.

5.1 Distribution of chlorine species

We first define three Cl families. The Cl_y family contains all gas phase inorganic species in the simulation (HCl, ICl, BrCl, ClNO₂, HOCl, ClNO₃, ClO, OCIO, Cl₂, Cl₂O₂, Cl and ClOO). Cl_{cycling} family which contains all gas phase inorganic species involved in cycling reactions (Cl_{cycling} = HOCl, ClNO₃, ClO, OCIO, Cl₂, Cl₂O₂, Cl and ClOO). Finally define a ClO_x family which represents the fast cycling between Cl and ozone (ClO_x = Cl, ClOO, ClO, OCIO and Cl₂O₂). Figure 5.1 shows the distribution of the Cl_y family and the most important Cl_y components (HCl, BrCl, ClNO₂ and ICl).



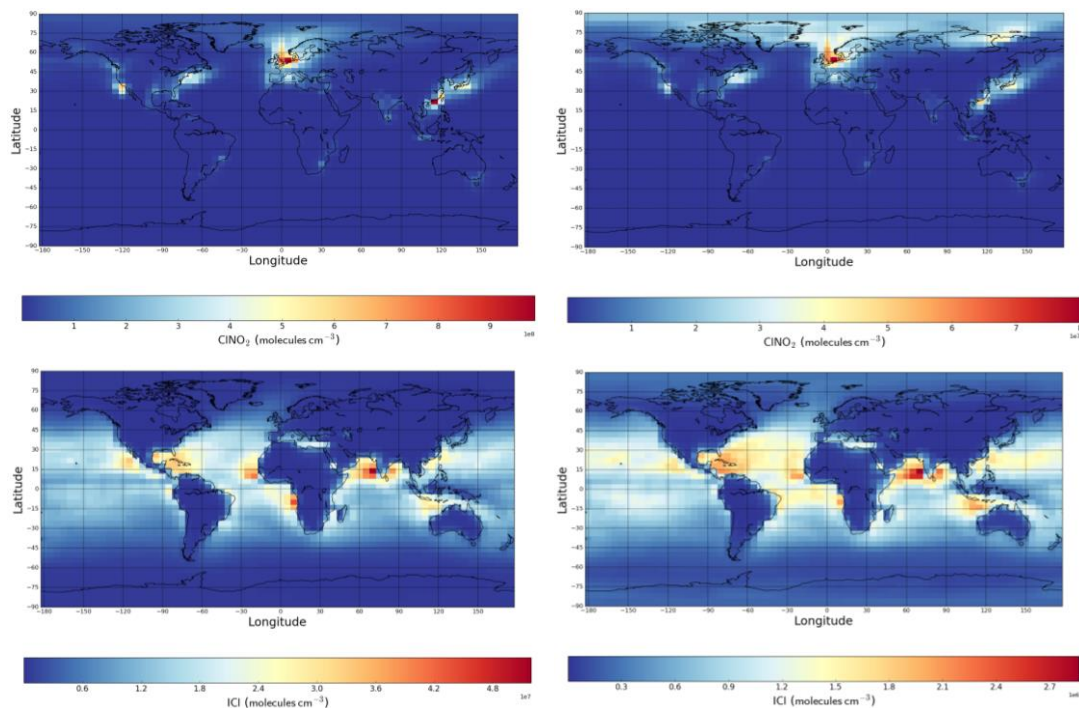


Figure 5.1 Concentrations of (from top to bottom) Cl_y , HCl, BrCl, ClNO_2 and ICl. Sea level concentration are on the left with whole column averages on the right.

At the surface, the highest Cl_y concentration are found over polluted marine locations such as the North Sea, the east and west seaboard of North America and coastal Asia. On average over the column concentrations are lower with generally zonal distribution of Cl_y . The highest concentrations are seen in the tropics around 30°N . This represents a region of downward transport of air in the Hadley circulation which brings high chlorine air (predominantly HCl) from the stratosphere down into the troposphere (see later section).

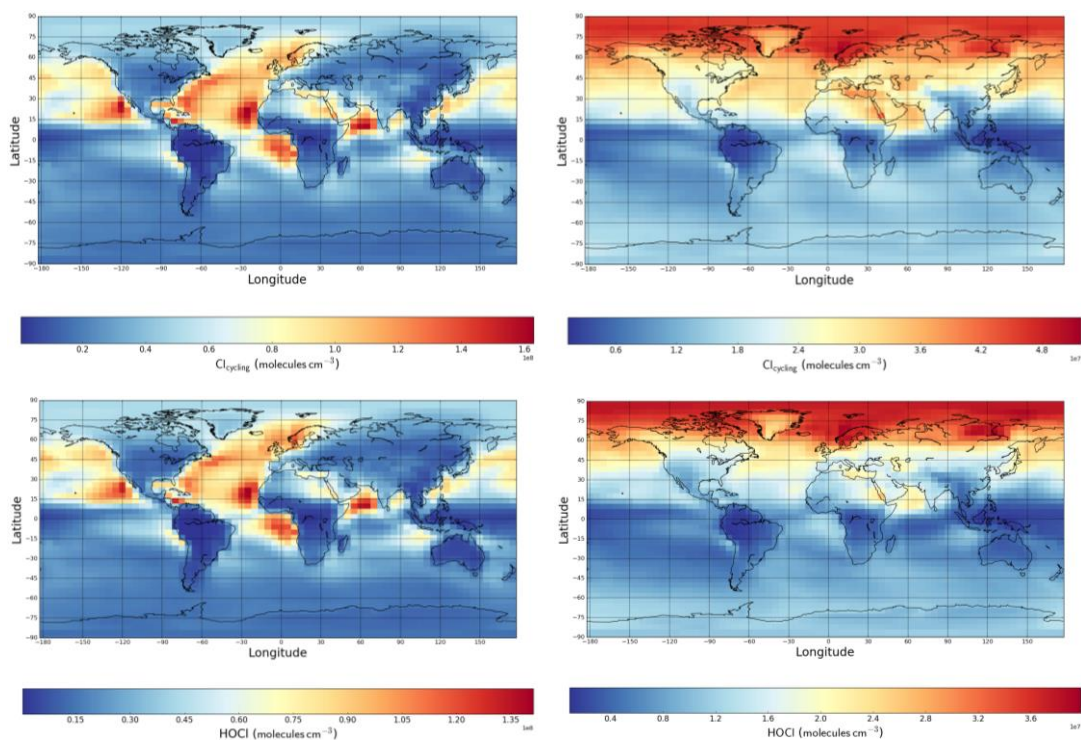
Surprisingly, surface HCl is highest over continental regions this is especially so over dry regions such as the deserts. This is reflecting two different processes. The first is that the HCl lifetime is longest in regions without rainfall. Thus, HCl has a much longer lifetime over dry, rainless regions than regions with high rain fall. Secondly in the current model parameterizations HCl is lost onto the surface of sea-salt aerosol alone. So over the ocean there is a sink for HCl to aerosol which does not exist over the land. Through the column the HCl distribution is dominated by the stratospheric signature of HCl descending from the stratosphere.

BrCl and ICl are produced mainly through the uptake of HOBr, BrNO_2 , HOI and IONO_2 onto sea salt (as discussed in Chapter 4). This heterogeneous mechanism accounts for 85% of the BrCl and 97% of the ICl at sea level. Gas phase production (from $\text{XO} + \text{YO} \rightarrow \text{XY} + \text{O}_2$) accounting for the remaining source. Thus at sea-level

BrCl and ICl thus have a strong dependence on sea salt aerosol concentration as shows in their distribution over marine regions (Figure 5.1). When averaged over the whole column the ICl maintains this marine character. However, BrCl becomes more evenly spread over the northern hemisphere. This is due to its production in the model on SO_4^{2-} aerosol which is fairly well distributed over the Northern Hemisphere. The model doesn't contain this reaction for ICl and so BrCl and ICl exhibit markedly different distributions in the column average.

The high concentrations of Cl_y seen in polluted marine environments is due to high concentrations of ClNO_2 . ClNO_2 accumulates over marine regions with high NO_x emissions due to its dependence on NO_x (N_2O_5) and sea salt concentration (reactions R1a - c), as such "hot spots" of ClNO_2 represent the areas of highest Cl_y concentration at sea level (Figure 5.1) ClNO_2 does not participate directly in Cl cycling being formed via N_2O_5 in the production route discussed in Chapter 4.

Attention is now drawn to the $\text{Cl}_{\text{cycling}}$ family. This represents the moderately fast cycling between species and essentially is the Cl_y family with the HCl removed as cycling of HCl back into other more reactive forms of Cl is slow. BrCl, ICl and ClNO_2 are also dropped as they are predominantly formed through primary production rather than cycling. Figure 5.2 shows the annual mean surface and column average concentration of $\text{Cl}_{\text{cycling}}$ and other components of this family.



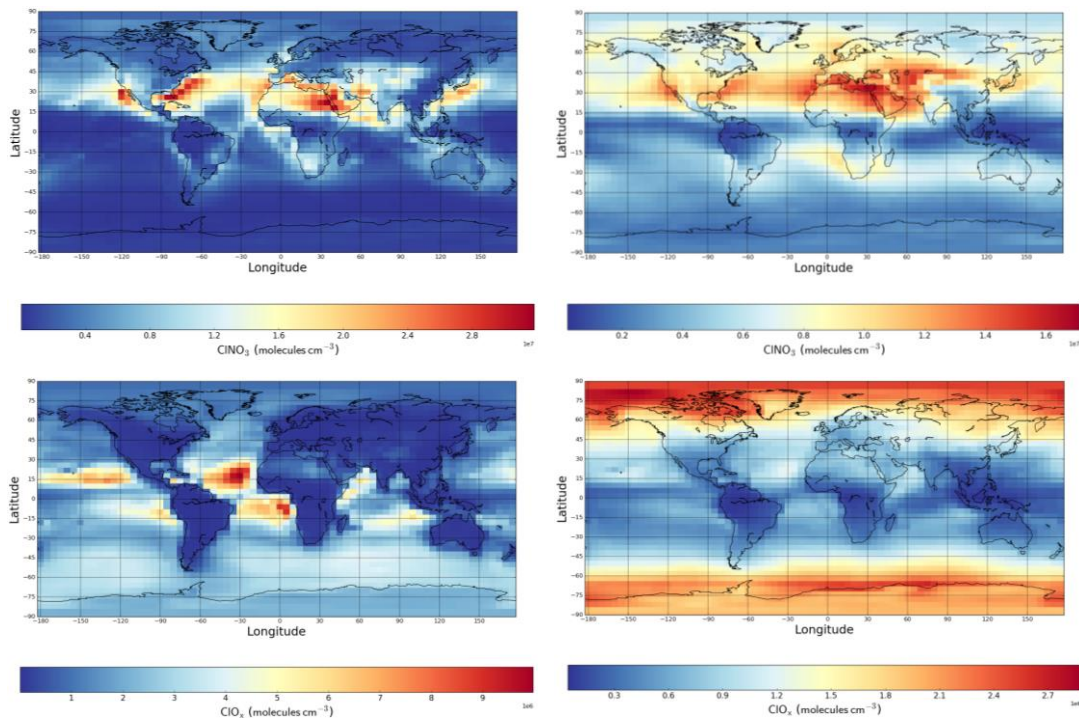


Figure 5.2 Concentrations of (from top to bottom) $\text{Cl}_{\text{cycling}}$, HOCl, ClNO_3 , and ClO_x . With sea level on the left and whole column average on the right.

At sea-level $\text{Cl}_{\text{cycling}}$ is made up predominantly of HOCl. This reflects its longer photolytic lifetime compared to other Cl species and its slow deposition rate. In the high sea-salt aerosol condition, ClNO_3 removal by sea salt aerosol is relatively rapid resulting in low concentrations of this compound.

Averaged over the whole column the spatial distribution of $\text{Cl}_{\text{cycling}}$ is a combination of HOCl and ClNO_3 with similar 10^7 cm^{-3} concentrations in the northern hemisphere (Figure 5.1). ClNO_3 is high in areas with high O_3 and NO_2 , thus the northern hemisphere dominance. HOCl accumulates in higher concentrations in the northern arctic, this is likely due to the high Cl content in the northern hemisphere coupled with the low rate of removal via photolysis and OH in the arctic.

Figure 5.2 also shows the distribution of the ClO_x family (ClOO , ClO , OCIO and Cl_2O_2). This family involves fast cycling of Cl with O_3 and thus a northern hemisphere dominance is expected as with HOCl the high concentrations in the arctic are likely due to slow removal rates.

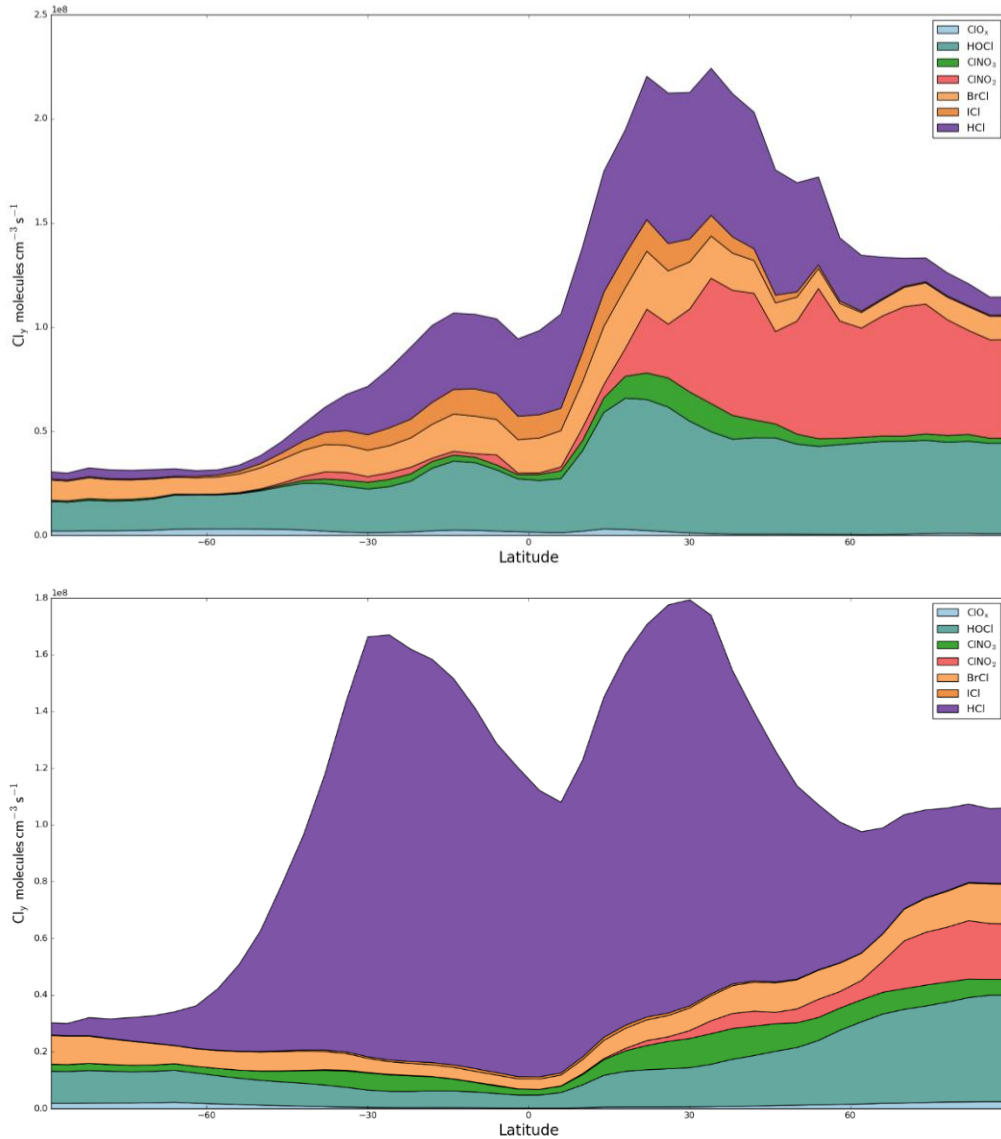


Figure 5.3a (top) and 5.3b (bottom) Figure 5.3 shows the speciation of Cl species in a zonal form at the surface (a) and averaged through the column (b).

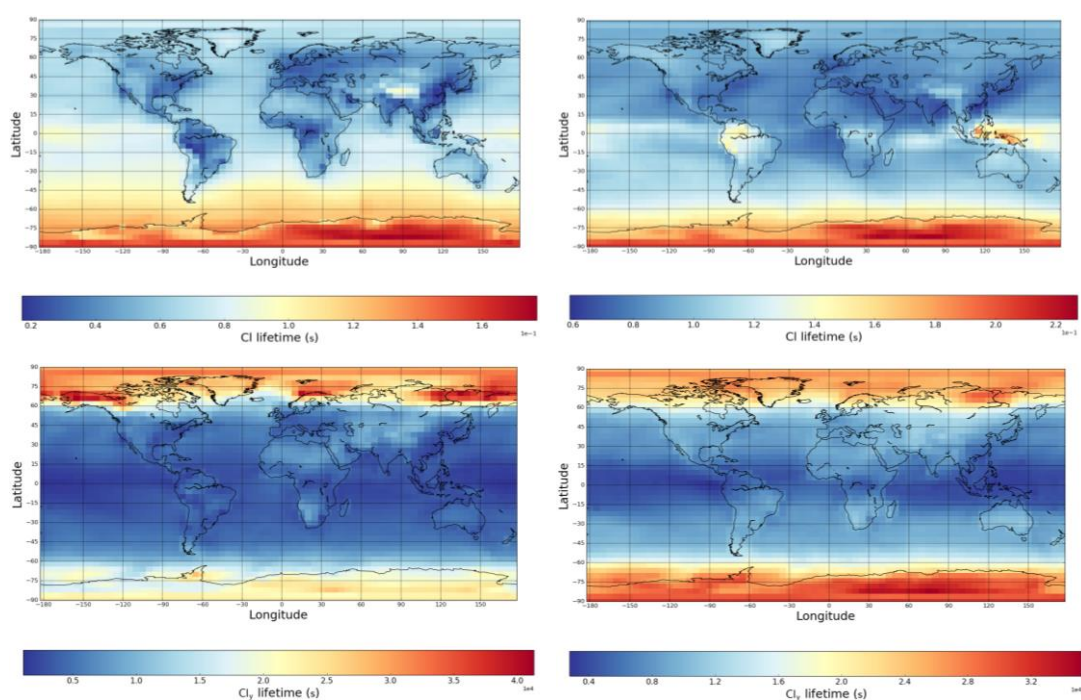
At sea-level there Cl_y is relatively equally spread between HCl (31%) and HOCl (29%) with the remaining Cl distributed between ClNO₂ (15%), BrCl (13%), ICl (7%), ClNO₃ (4%) with the remaining Cl distributed through the ClO_x family (ClO, Cl etc). However, there are distinct differences between the Northern and Southern hemisphere. ClNO₂ plays an almost insignificant role in the Southern Hemisphere but is very significant in the Northern Hemisphere where it is the dominant Cl_y species. This reflects the significantly higher NO_x emissions in the Northern Hemisphere compared to the Southern Hemisphere which can form the N₂O₅ needed to generate the ClNO₂ through heterogeneous reaction on sea-salt.

Globally averaged the distribution of Cl_y is significantly different than at sea level (5.3b). Globally, Cl_y is composed of 80.9 % HCl, 7.9 % HOCl, 4.7 % BrCl, 4.2 % $ClNO_3$, 1.6 % ClO_x , 1.2 % $ClNO_2$ and 0.5 % ICl. Thus, nearly all of the Cl_y is in the form of HCl and is thus chemically very inert. This reflects the much lower aerosol surface area in the column compared to the surface meaning that heterogeneous reactions that can produce chlorine or can recycle HCl into more active forms are much slower averaged over the column than they are at the surface.

These interconversion reactions are key to understanding the chemistry controlling the concentration of Cl in the atmosphere. Attention now turns to this cycling.

5.2 Cycling between species

In the introduction chapter the chemistry of chlorine used in the model is described, with the most prominent pathways in bold. This describes the interconversion routes which are possible between species. Here we investigate the routes for conversion between different families of chlorine species and the routes for conversion within families. One mechanism to understand this interconversion is to explore the lifetime of different components of the Cl system. These lifetimes are shown in Figure 5.4 again at the surface but also averaged through the column.



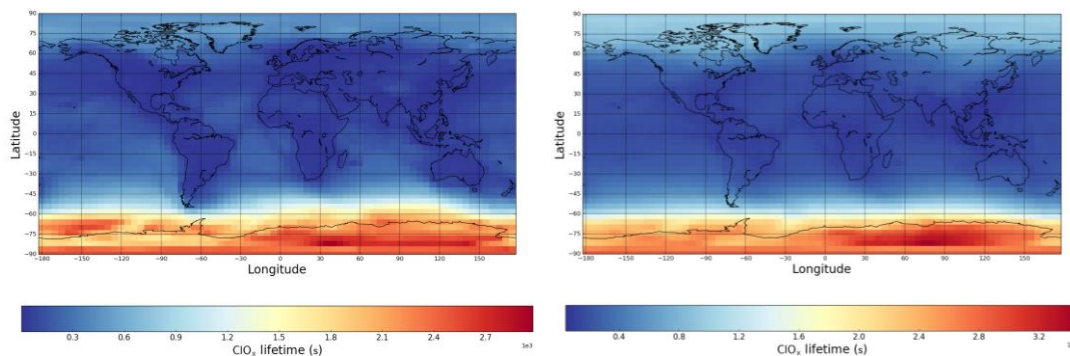


Figure 5.4 Lifetime of (from top to bottom) Cl, Cl_y and ClO_x. With sea level on the left and whole column average on the right. The fast cycling between Cl and O₂ to form ClOO has been excluded from the Cl the lifetimes calculated here.

The total Cl_{cycling} lifetime is the amount of time Cl remains active in the troposphere before Cl is removed into the HCl reservoir. Cl cycling has a lifetime of around 2.5 hours averaged over the whole column, at sea level the lifetime drops to just over 1 hour. Due to the short lifetime of Cl cycling, Cl_{cycling} will experience only minimal transportation thus Cl removal will be regionally specific with areas experiencing greater production experiencing greater removal, as such regions with inflated Cl would be expected to have increased VOC removal via Cl and this will be looked into in section 7.

HOCl represents 81.5 % of Cl_{cycling} species at sea level with a life time of over 4 hours with respect to cycling reactions, over the whole column the life time drops to under 4 hours and HOCl represents 60.5 % of the Cl_{cycling} species.

ClNO₃ represents 11.5 % of Cl_{cycling} species at sea level with a lifetime of just over an hour with respect to cycling reactions, however when averaged over the whole column the lifetime increases to nearly 4 hours and represents 33.5 % of the Cl_{cycling} species in the troposphere. This increase in lifetime is due to ClNO₃ removal via sea salt aerosol dying of rapidly with altitude. 13.5 % of ClNO₃ is recycled back into Cl via BrCl, however in this study BrCl component of cycling as only 3% of tropospheric BrCl is produced via ClNO₃.

The ClO_x lifetime is much longer ClO_x lifetime is < 5 mins due to cycling ending via reaction with OH, IO or NO_x. The exception is arctic where it increases to ~15 minutes in the north and ~ 45 mins this is likely due to the higher NO_x concentration in the northern hemisphere.

5.3 Cl_y sinks

HCl is the main removal route for Cl_y due to its high rate of wet deposition. Once Cl has entered the HCl reservoir it is essentially no longer chemically active, unless reactivated via either OH or HOBr on aerosol surfaces. OH reaction with HCl has a relatively low rate of reaction, with HCl having a lifetime of 11 days with respect to OH. With respect to HOBr, HCl has a tropospheric lifetime of 22.5 hours with this lifetime falling to 15.5 hours in the northern hemisphere. As such HCl can be seen to have a sink vs reservoir nature with it acting more like a reservoir when the rate of the HOBr reacting with HCl on aerosol increase and acting as a sink away from significant HOBr concentrations.

Wet and dry deposition compete effectively with the recycling of HCl into more active Cl species. Thus 85% of the ultimate Cl_y loss occurs through the wet and dry deposition of HCl. Wet and dry deposition of HOCl and ClNO₃ can also act to remove Cl_y from the troposphere but these are small sinks compared to HCl deposition accounting for 11 % and 3.2 % of Cl_y removal respectively.

5.4 Chapter Summary

The distribution of reactive chlorine species in the model is complex. Globally the dominant Cl_y species is HCl but in the boundary layer and the northern hemisphere other compounds (notably ClNO₂) can play a significant role in the composition of Cl_y. The distribution is controlled, to a large extent, by the emissions of other compounds (NO_x, VOCs etc) but it is ultimately the heterogeneous processing which determining the ratio of HCl to more active Cl_y components. And it is ultimately the degree of these active chlorine compounds (ClO_x) which determines the amount of atomic chlorine in the atmosphere. Central to this is the rate of removal of Cl to form HCl which essentially determines the lifetime of active chlorine in the atmosphere. In the next chapter we will look into the routes for Cl_y to enter the HCl reservoir. We will then look into the potential size of the Cl sink for a variety of VOCs

6. Atomic Chlorine Sinks and Atmospheric Oxidation

As discussed in Chapter 5 the predominant removal route reactive chlorine in the troposphere is via wet deposition of HCl. The dominant route for the production of HCl is through the reaction with atomic chlorine with VOCs. In this chapter, we examine the different VOCs that atomic Cl reacts with to form HCl (Section 6.1) and then how the route compares to that of the hydroxyl radical for the removal of VOCs (Section 6.2 and 6.3).

6.1 Cl removal routes

Methane is the most prominent species to remove atomic Cl with 44.1 % being removed via this species. Oxygenated volatile organic compounds remove a large portion of atomic Cl, with the largest being alcohols (methanol and ethanol) removing 14.8 %, followed by methyl hydro peroxide, formaldehyde, acetone, carboxylic acids (formic and ethanoic) at 12.3, 7.7, 7.0 and 6.2% respectively. Ethane, propane and amalgamated longer alkanes (ALK4) account for 6.5, 2.1 and 4.5 % respectively. VOCs which consists of amalgamated alkenes (PRPE), and isoprene making up approximately 1 % each.

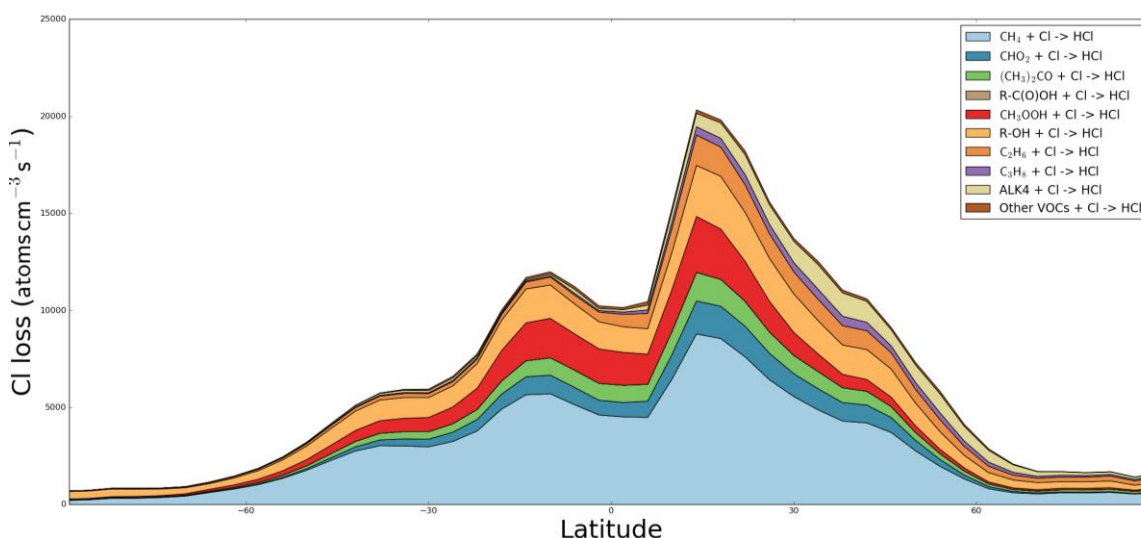


Figure 6.1 shows the zonal mean rate of loss of atomic Cl by reaction with VOCs at sea-level.

When considered for the whole tropospheric column the story remains the same (Figure 6.2). Methane remains the largest sink at (44.2 %) with the role of the alkanes increasing due to their longer lifetime with respect to the other more reactive VOCs (C_2H_6 8.4 %, C_3H_8 2.2 % and ALK4 3.7 %).

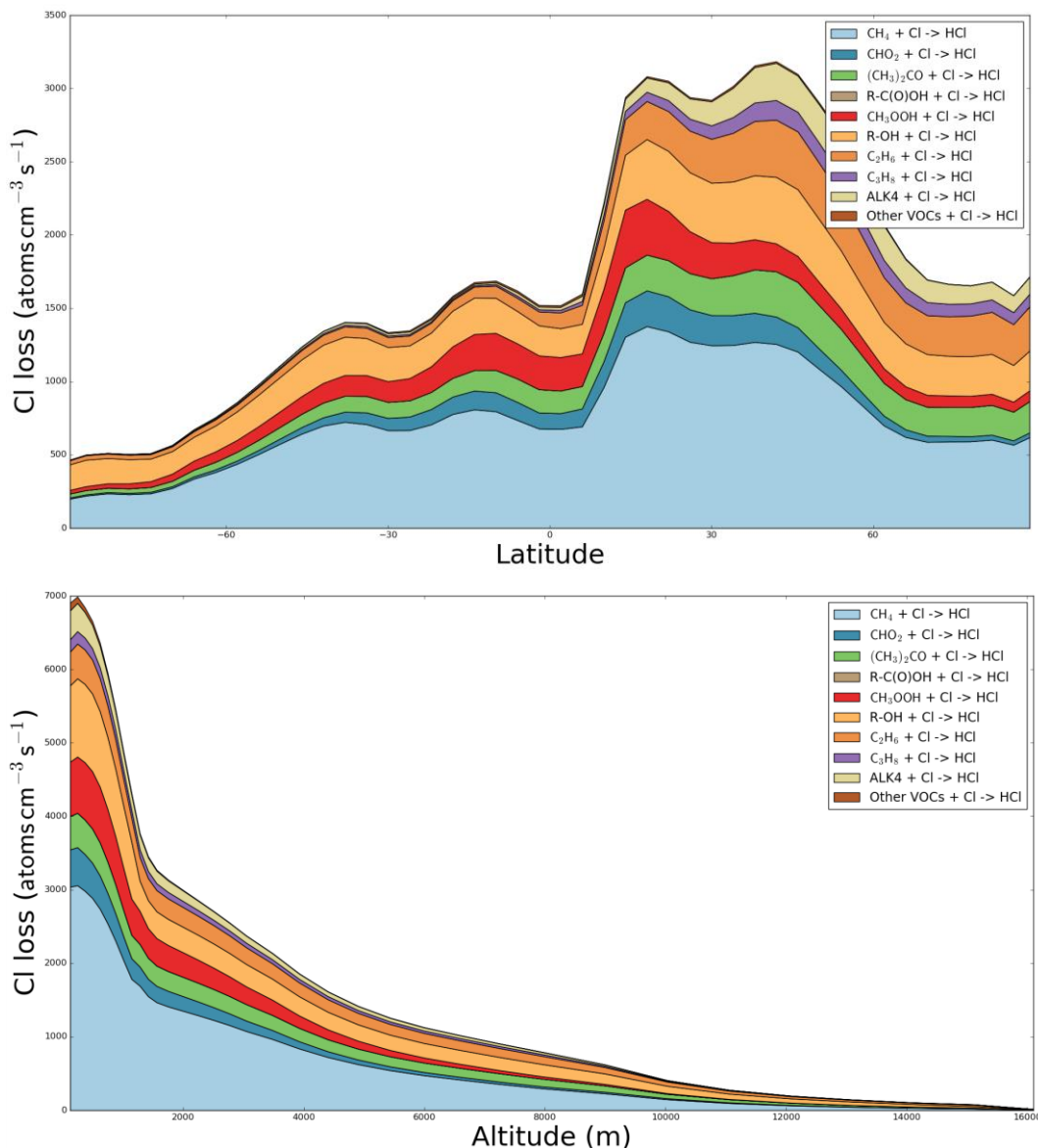


Figure 6.2a(top) and 6.2b(bottom) whole column zonal plot loss of atomic Cl(a), plot of loss by altitude(b).

As discussed in the previous chapter this removal results in Cl_{cycling} having a lifetime of 1 hour at sea level increasing to 2.5 hours averaged over the whole column.

Much like OH atomic Cl is removed via its reaction with a range of different VOCs, however this process also removes the VOCs in question. As such we will now investigate how removal via reaction with Cl compares to removal via OH (the most important atmospheric VOC removal process) for all of the alkanes in section 6.2, and then specifically for ethane and OVOCs in 6.3.

6.2 Removal of alkanes

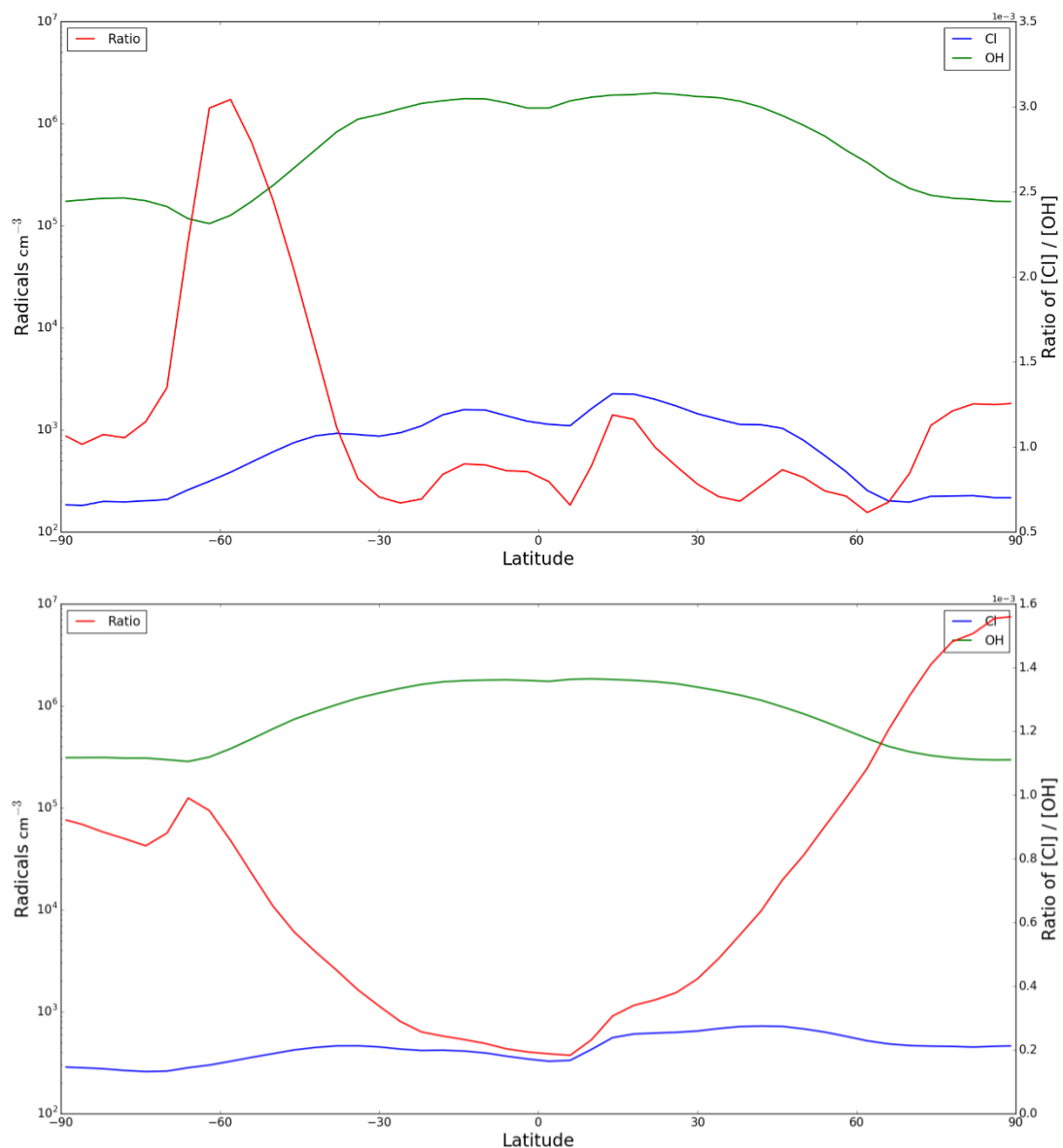


Figure 6.3a (top) and 6.3b (bottom) the zonal average Cl and OH concentrations and the ratio, both at the surface (a) and through the column (b).

The removal of alkanes from the atmosphere is initiated by their oxidation from OH and Cl. It is clear from Figure 6.3 that OH is present in the order of 3 magnitudes higher concentration than Cl. However, moving across latitudes the ratio between the two varies substantially, over the column averaged Cl/OH ratio being 8 times higher over the higher latitudes, this reflects OH production being reliant on sun light intensity compared to Cl which has a strong sea-salt component (as discussed in chapter 4).

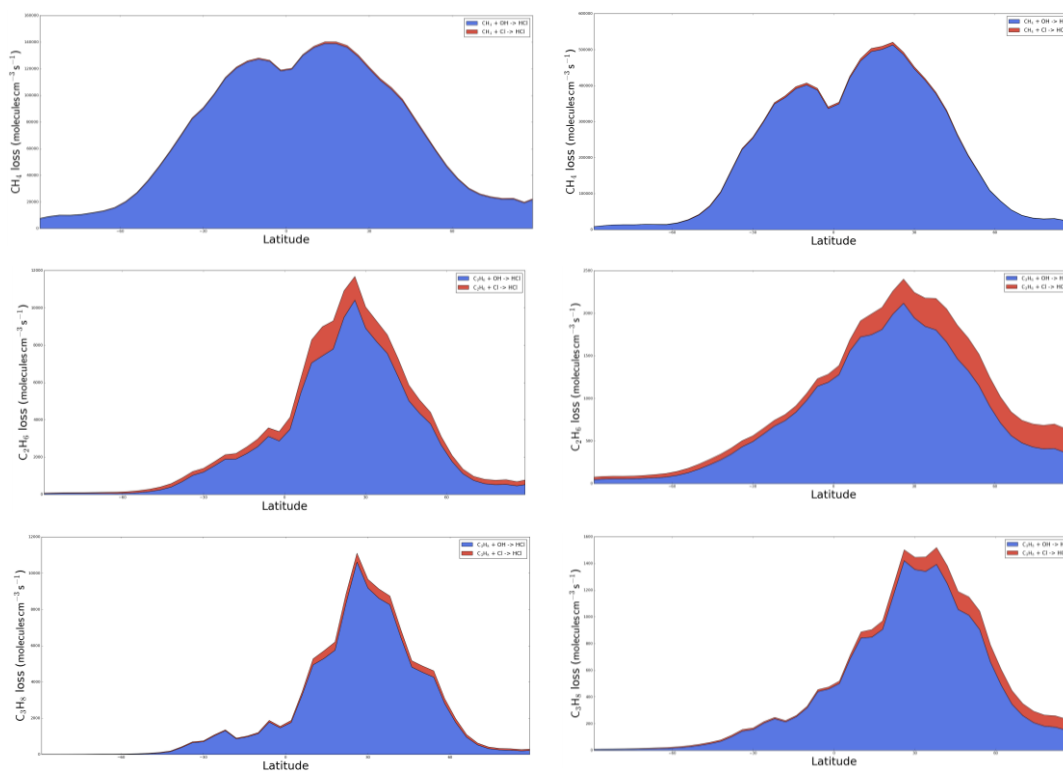
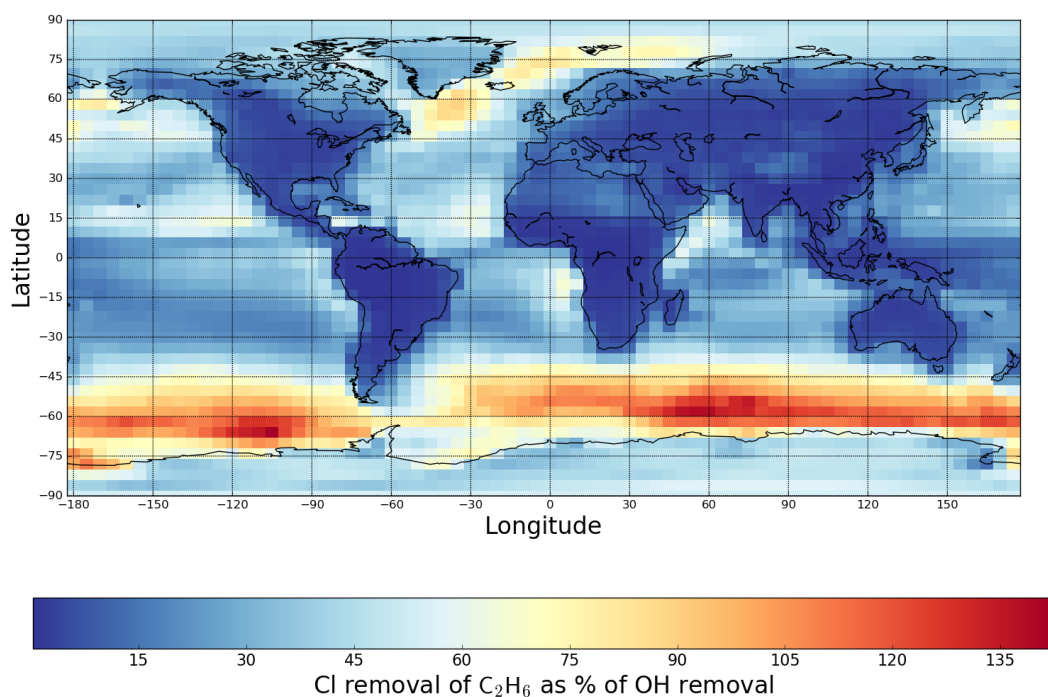


Figure 6.4a-b (top), c-d (middle) and e-f (bottom) shows the zonally averaged removal sea-level (left) and whole column (right) methane (top), ethane (middle) and propane (bottom).

At sea level the Cl methane sink is ~1.4 % the size of the OH sink with this falling to 0.9 % over the whole column (Figure 6.4b). Cl is a small sink for methane in the model. This reflects that much lower average Cl concentration in the model (495 Cl atoms cm³) compared to OH (1.27 × 10⁶ cm⁻³) despite the substantially (15 times) faster reaction rate between methane with Cl compared to OH. The total size of the Cl methane sink was calculated to be 4.67 Tg yr⁻¹ this is comparable to the ~1 % of removal found by Sherwen et al., (2016) and about half the value found by Hossaini et al., (2016) (~2.5 %).

Cl removes a more significant fraction of the ethane (see Figure 6.4c-d) than for methane. At sea level, Cl removes 16.3 % ethane with this dropping to, 15.0 % over the whole column (Figure 6.4d). This large removal of ethane by Cl is due to its rate constant with Cl. Figure 1.1 shows, for a range of hydrocarbons, their rate constant for reaction with Cl divided by their rate constant for reaction with OH (at STP). Ethane has the greatest ratio between Cl and OH rate constants, with the Cl rate being 228 times greater. As such ethane is the VOC most effected by tropospheric atomic Cl. Due to the regional variability in the atomic Cl concentrations (see Chapter 3), the ethane removal also varies spatially (Figure 6.4a) with higher

removal rates seen in marine and polluted regions. At sea level over marine regions where the Cl concentration is substantially higher due to the concentration of sea salt aerosol the removal rate is approximately 30% rising to near 50% in the polluted northern hemisphere. In the Southern Ocean although insignificant amounts of C_2H_6 are removed, Cl becomes the dominant removal species (+120% of OH), this is due to the latitude being entirely marine with a high wind speed (sea salt aerosol concentration is coupled to wind speed as discussed in Chapter 2), the spike in Cl is clearly seen in Figure 6.1a. Averaged over the whole column (Figure 6.5b) removal in the northern hemisphere marine regions falls to 20% of the OH removal, however unlike at sea level this percentage is seen over much of land mass as well. At the high latitudes removal increases to up to 80% this is reflective of the high $[Cl]/[OH]$ seen in these regions. The total size of the Cl ethane sink is 1.73 Tg Yr^{-1} .



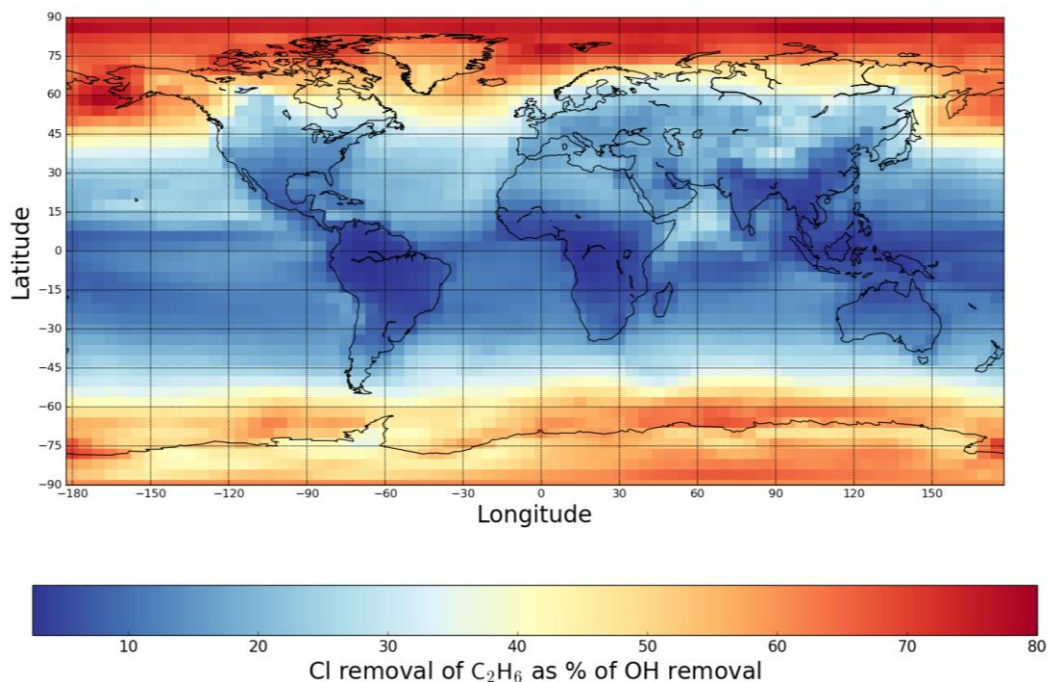


Figure 6.5a (top) and b (bottom) C_2H_6 removal via Cl as % of OH at sea level (a) and averaged over the column (b)

As suggested by Figure 1.1(rate contents vs VOC) at sea-level Cl plays a smaller role in the oxidation of propane sink (7.6 % of total) (Figure 6.2e), and 6.5% over the whole column (Figure 6.4f) with a total size of the Cl propane sink being calculated as 0.64 Tg Yr^{-1} .

Both ethane and propane removal rates are comparable to the ~9-18 % described by Sherwen et al., (2016).

Overall GEOSChem has been found to perform well replicating the special distribution of Ethane and Propane, except for an over estimation of between 20 – 30 % in Europe (Xiao et al. 2008), the high Cl resulting from production via $ClNO_2$ may help to explain this, would benefit from further study.

Table 6.1 Summary of removal of the C1 to C3 alkanes.

	Removed Via OH (Tg yr^{-1})	Removed Via Cl (Tg yr^{-1})
Methane	462	4.67
Ethane	9.80	1.73
Propane	9.21	0.64

6.3 Other VOCs

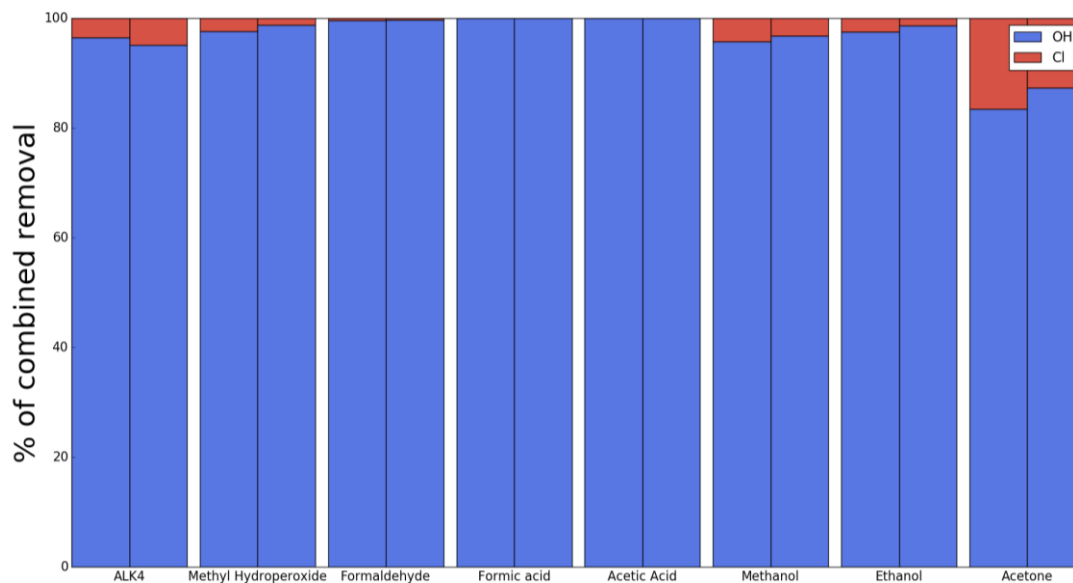


Figure 6.6 Comparison of VOC removal via OH and Cl, averaged over sea level (left column) and whole column (right column).

These species while important as sinks for atomic Cl, atomic Cl is not an important sink for them. As with methane this is due a small ratio between the Cl and OH rate constants, relative to the concentration difference. The exception is acetone, as it has a smaller Cl/OH ratio (11.5 times) than CH₄, and yet Cl accounts for 12.7 % of acetone removal over the whole column.

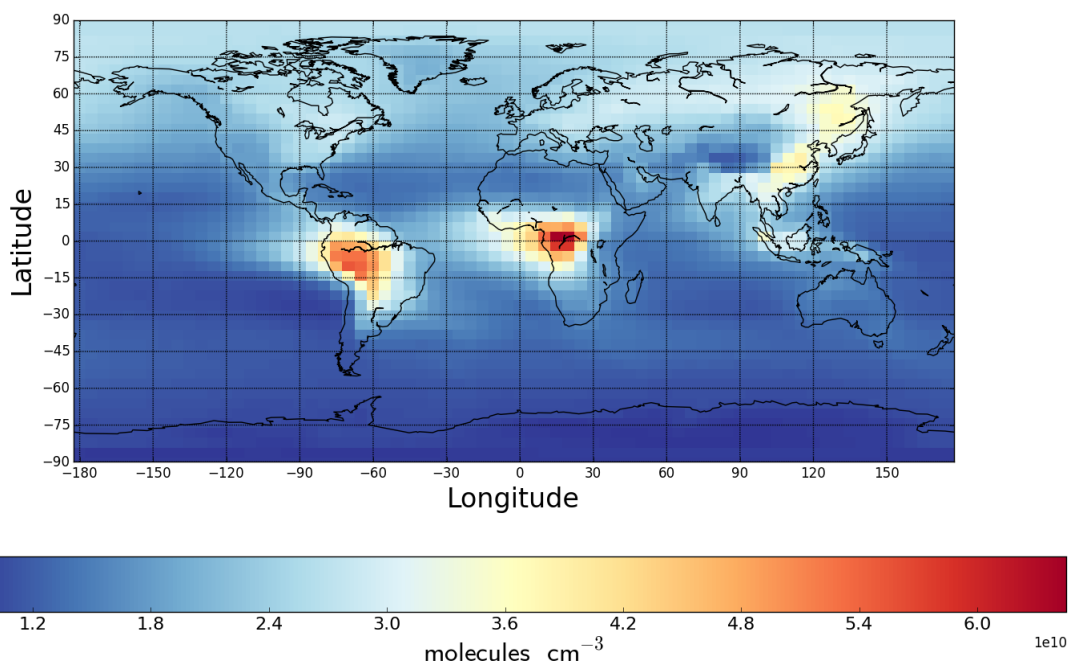


Figure 6.7 Spatial distribution of acetone over whole column.

In this simulation (Figure 6.7) acetone has a different special distribution to the predominantly anthropogenic alkanes and appears to be mainly focused in forest/jungle regions (as was seen in a study in 2015 by Khan et al.,) which are regions with low atomic Cl. As such the cause of the inflated removal via Cl is not obvious and will require further study.

6.4 Summary

Most previous studies (Lary 2004, Allan et al., 2007 and Thornton et al., 2010) have focused on the effect of Cl on the budget of methane. However, in these studies and in recent studies (Sherwen et al., 2016) this appears to be a small to insignificant sink at compared to that of OH (0.9 %). However, for other VOCs the story is more complicated. Within the model, Cl provides a significant sink for ethane constituting 15%, and it provides a reasonably large sink for propane (6.5%).

There is a high degree of regional variability with Cl removal of ethane, with the removal rising over the northern hemisphere oceans to ~50 % of OH removal at sea level and ~30 % averaged over whole column.

Outside of the tropics the relative role of atomic chlorine as an oxidant increases as the OH concentration decreases. Thus in the polar regions ethane oxidation is almost equal between OH and Cl in the annual mean. The low OH concentrations, and small surface areas of the polar region means that from the perspective of the global ethane burden this is not significant but from a regional perspective it is notable that chlorine can play such an important role.

As Cl oxidation represents a significant sink for ethane and propane in regions of high NO_x, it is likely this will influence the production of O₃ due to the reduction in VOC precursor. As such it would be useful to include Cl + ethane and Cl + propane reaction in models/simulations used to predict tropospheric ozone.

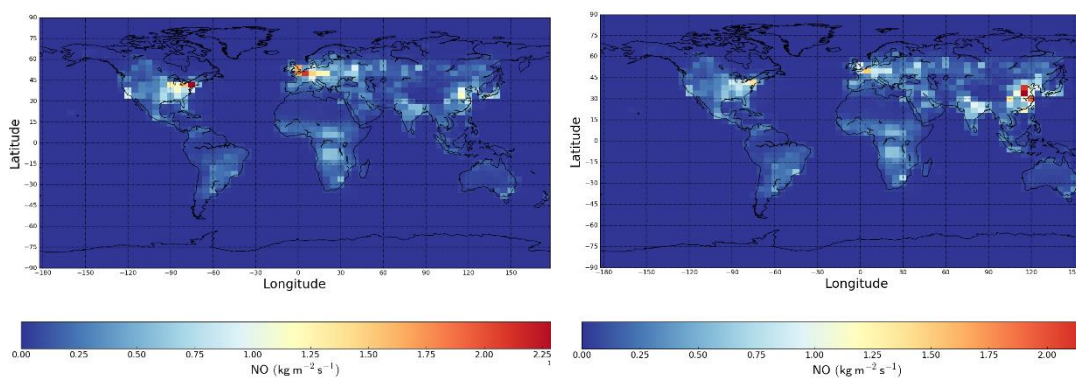
It is evident that, within the model, atomic chlorine can play a role in the oxidizing capacity of the atmosphere. In the next section, the change in atomic Cl concentrations as anthropogenic emissions changed between 1988 and 2008 is explored.

7. Chlorine Distribution Change 1988 to 2008

Over the last three decades the emission of primary pollutants has moved from the developed to developing regions (Zhang et al., 2016) and so from the northern mid-latitudes towards the tropics. This has been shown to lead to an increase in the tropospheric O₃ burden (Zhang et al., 2016). In this chapter the impact on atomic chlorine concentrations is investigated. The model is run nominally for 2008 with 1988 emissions and for 2008 with 2008 emissions, spinning up with 1987 and 2007 respectively and discarding this data to prevent any influence from the initial conditions. To remove the variability due to meteorology in these years the same meteorology is used (2008) for both simulations. The EDGAR emissions (<http://edgar.jrc.ec.europa.eu/>) describe the emissions over this period and these emissions are used in this study to describe the changes in anthropogenic emissions. Other non-halogenated emissions (biomass burning, soil NO_x, isoprene, lightning etc.) remain the same. Halogen emissions have no annual variability and thus will not change between simulations. In Section 7.1 the changes in the emissions used in the model over this period are described. In Section 7.2 the resulting changes to the concentration of non-chlorine compounds are outlined and finally in Section 7.3 the change in the concentration of chlorine compounds in the simulation is described.

7.1 Emissions changes

The v4.2 EDGAR emissions attempt to describe the changes in emissions over the period of 1970 to 2008. We explore the change between 1988 and 2008 emissions. CH₄ concentrations in the simulation are fixed to the appropriate observational values for 1988 and 2008 (Dlugokencky et al., 2016). Figures 7.1-7.7 show the emissions used in 1988 and 2008 and the fractional increase over this period for NO, CO, SO₂, C₂H₆, C₃H₈ and other VOCs.



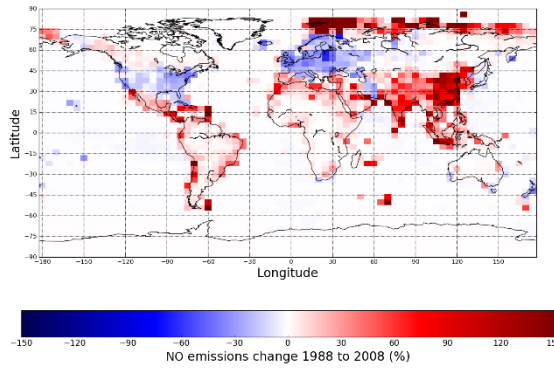


Figure 7.1 NO emissions in 1988 (top left) 2008 (top right) and the change in percentage (left).

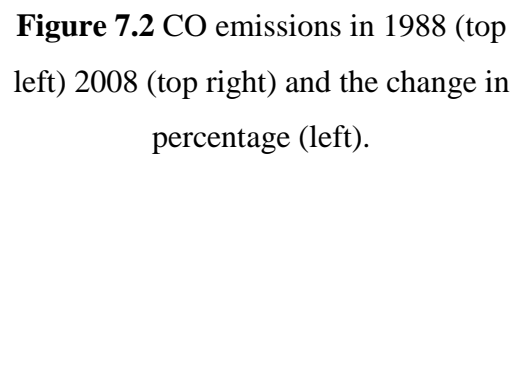
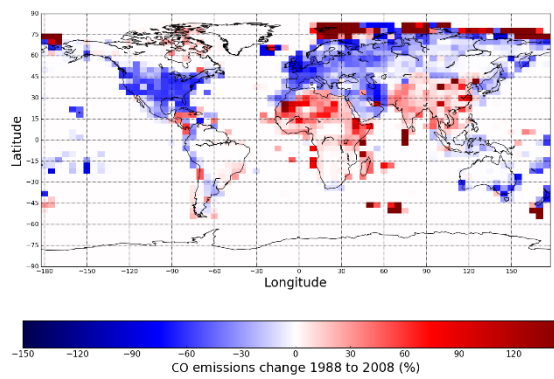
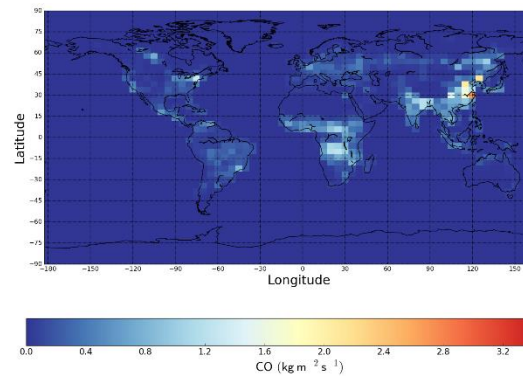
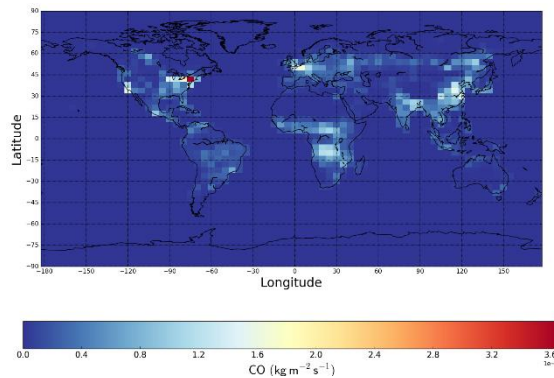
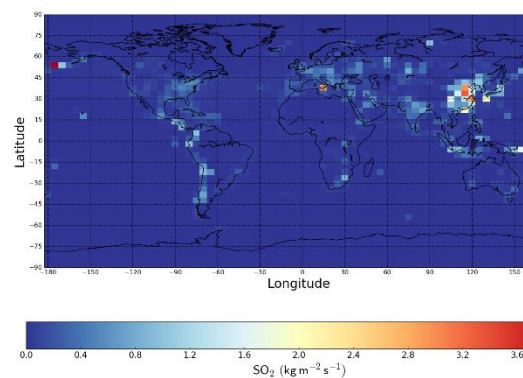
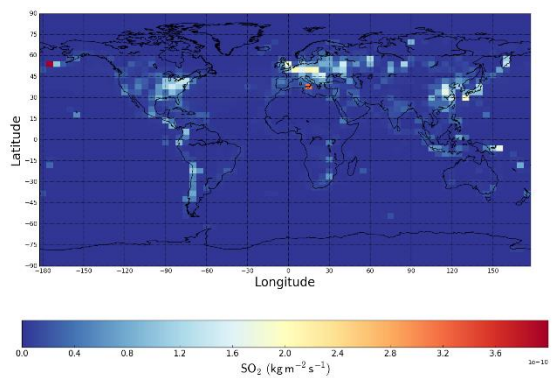


Figure 7.2 CO emissions in 1988 (top left) 2008 (top right) and the change in percentage (left).



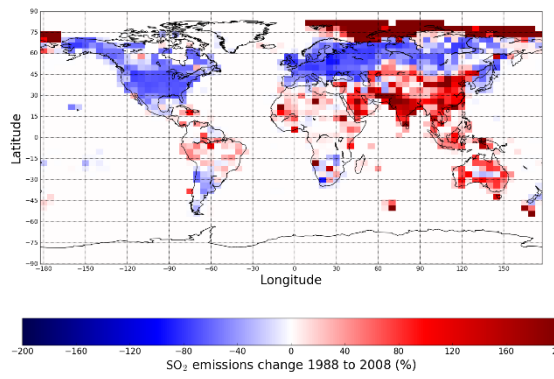


Figure 7.3 SO₂ emissions in 1988 (top left) 2008 (top right) and the change in percentage (left).

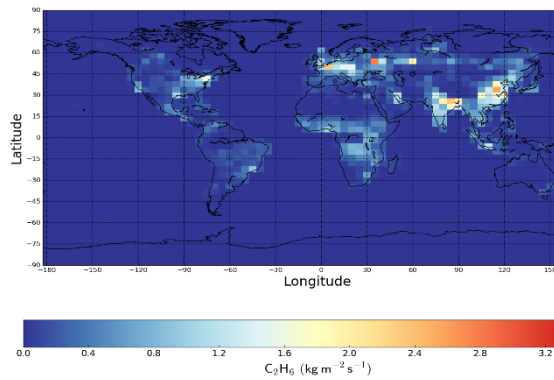
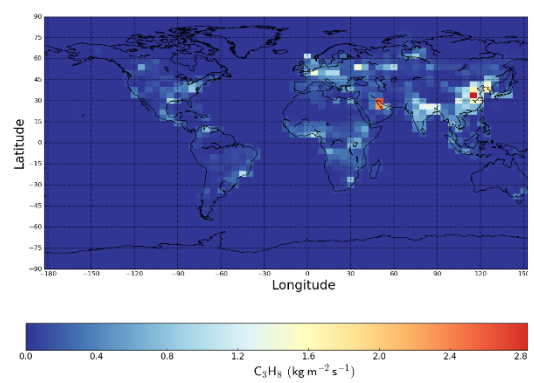
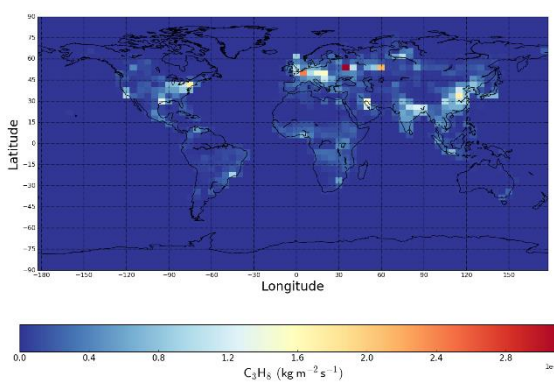
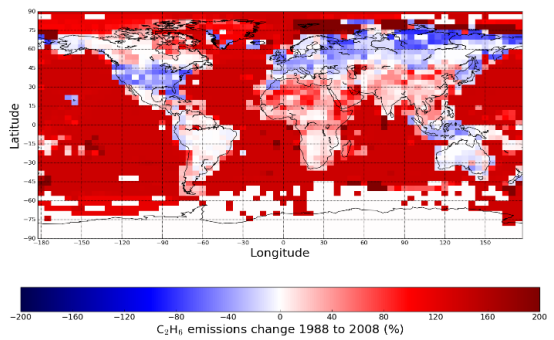


Figure 7.4 C₂H₆ emissions in 1988 (top left) 2008 (top right) and the change in percentage (left).



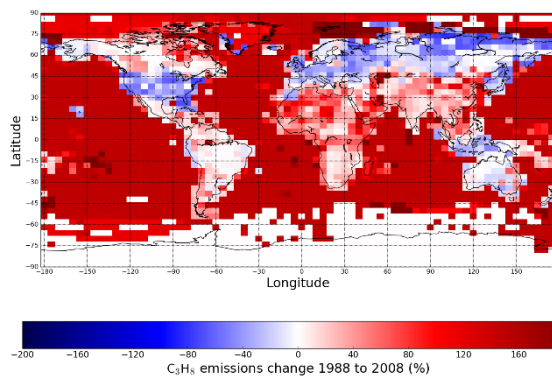


Figure 7.5 C_3H_8 emissions in 1988 (top left) 2008 (top right) and the change in percentage (left).

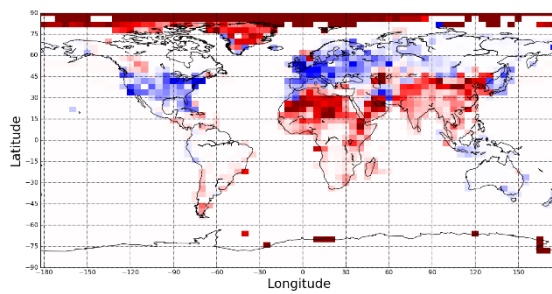
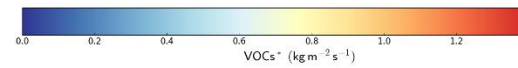
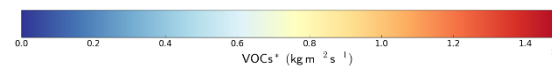
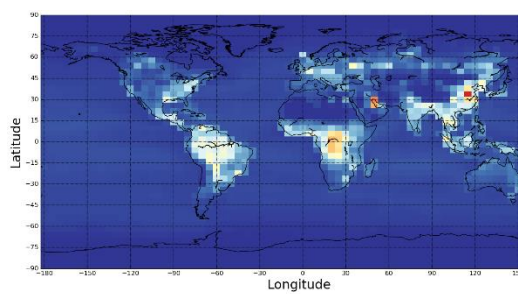
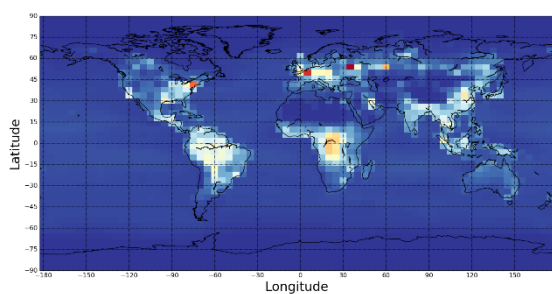
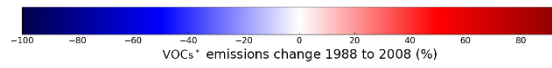


Figure 7.6 Combined CH_2O , acetone, C_4+ alkanes and acetaldehyde emissions in 1988 (top left) 2008 (top right) and the change in percentage (left).



In general, the emissions of pollutants drop over North America and Europe reflecting efforts in these countries to implement pollution control measures to reduce air quality pollution (Vestreng et al., 2008 and Helmig et al., 2016). For some compounds, such as SO_2 , where technology exists to reduce pollution and the pollution leads to a significant public health issue this has led to very large reductions ($\sim 80\%$). For other compounds such as NO_x the reduction has been more muted ($\sim 20\%$).

Over some developing regions (China, India, South America) the trend has been in the opposite direction. Increasing populations coupled to industrialization has led to significant increases in the emissions of primary pollutants from these regions. (Ohara et al., 2007). SO_2 , NO_x , VOC emissions may have doubled in some of these

regions reflecting massive increases in the burning of hydrocarbons associated with industrial and domestic activities.

Ethane (Figure 6.4) and propane (Figure 6.5) emissions can be seen to increase by a large factor in marine regions in the order of 150 to 200 %. This is a result of increased marine activity globally however this does not represent a large increase in emissions in absolute terms.

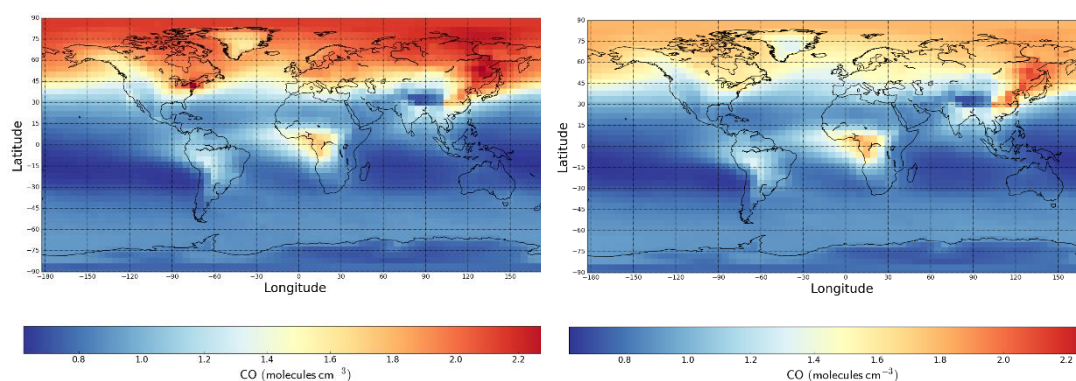
These changes in the emissions over this period have led to changes in the concentration of pollutants around the world. In the next section these changes are explored in the model.

7.2 Impact on non-halogenated species

The changing of emissions of the primary pollutants leads to changes in the concentration of these primary pollutants but also in many of the secondary component of the atmosphere. The changes for the primary species are investigated first (Section 7.2.1), followed by key non-chlorinated species (Section 7.2.2) and finally the impact on chlorinated species are investigated (Section 7.2.3).

7.2.1 Primary species

The concentration of primary pollutants largely follows the same trends seen in their emissions. However, due to the lifetime of the pollutants in the atmosphere (hours-weeks) and the global mixing patterns the changes tend to fall into two regions – decreases over the northern mid-latitudes and pole, and increases over the tropics and southern hemisphere.



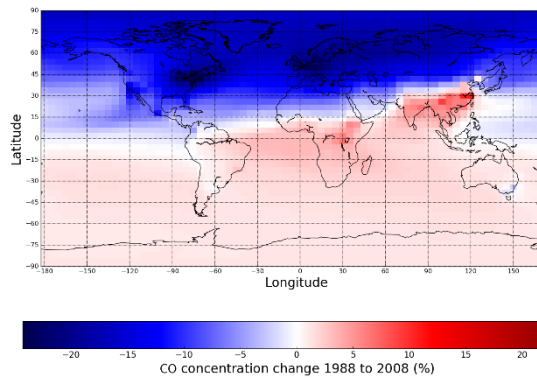


Figure 7.7 CO whole column average concentration in 1988 (top left) 2008 (top right) and the change in percentage (left).

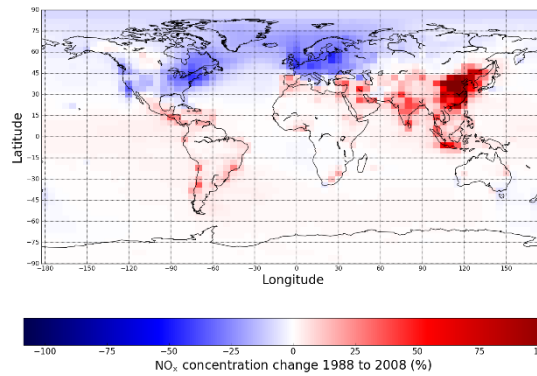
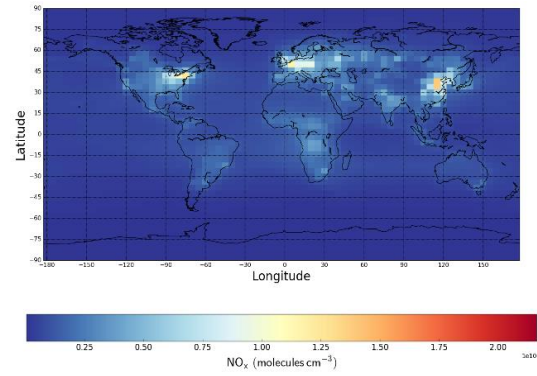
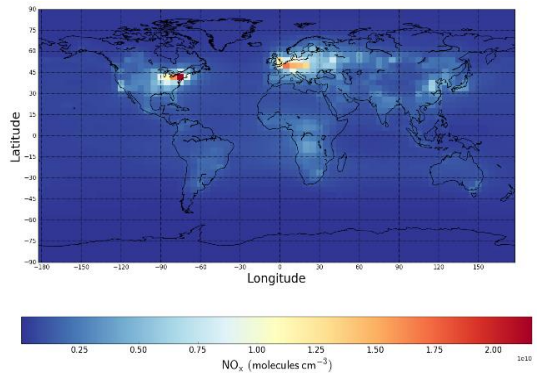
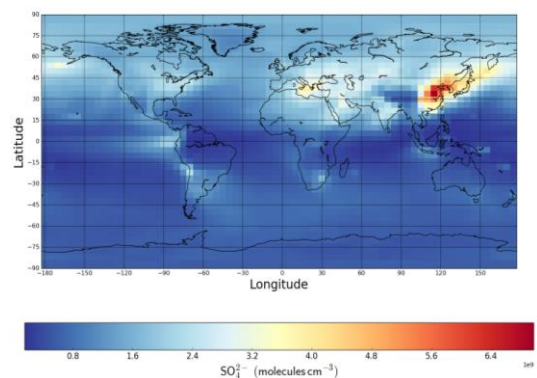
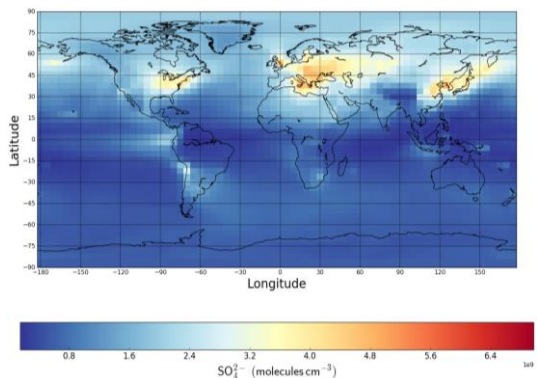


Figure 7.8 NO_x whole column average concentration in 1988 (top left) 2008 (top right) and the change in percentage (left).



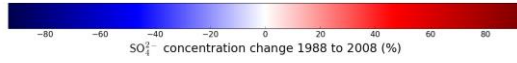
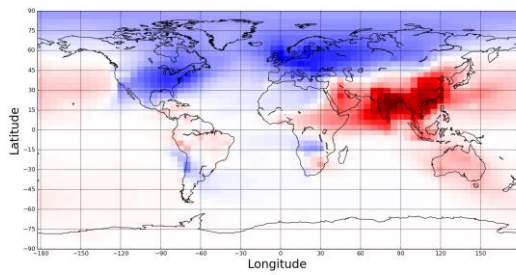


Figure 7.9 SO_4^{2-} whole column average concentration in 1988 (top left) 2008 (top right) and the change in percentage (left).

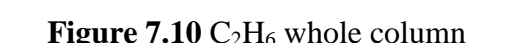
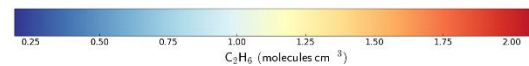
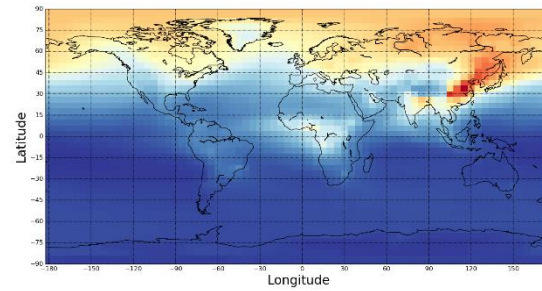
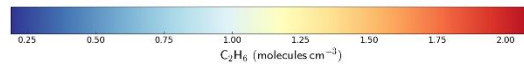
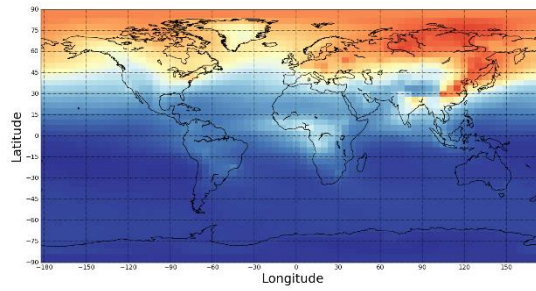
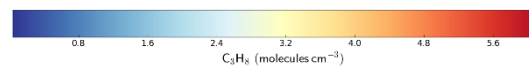
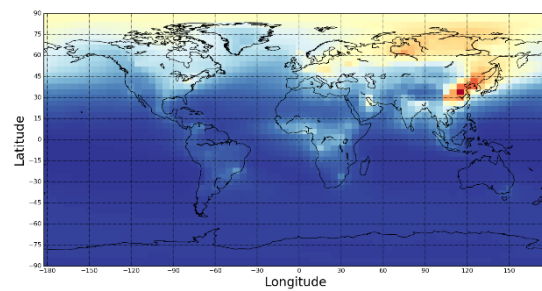
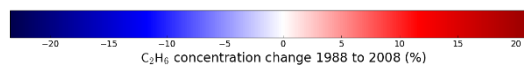
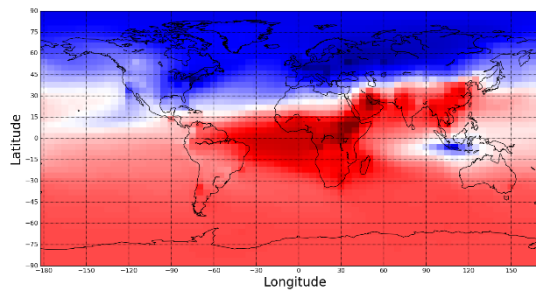


Figure 7.10 C_2H_6 whole column average concentration in 1988 (top left) 2008 (top right) and the change in percentage (left).



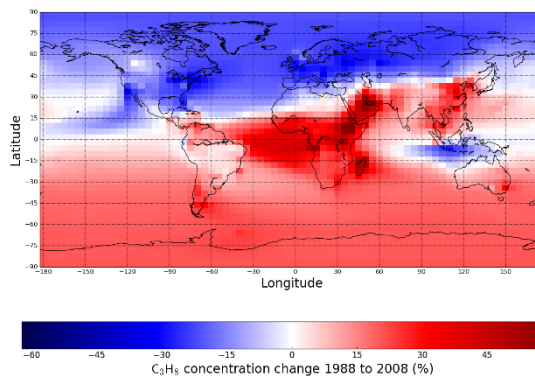
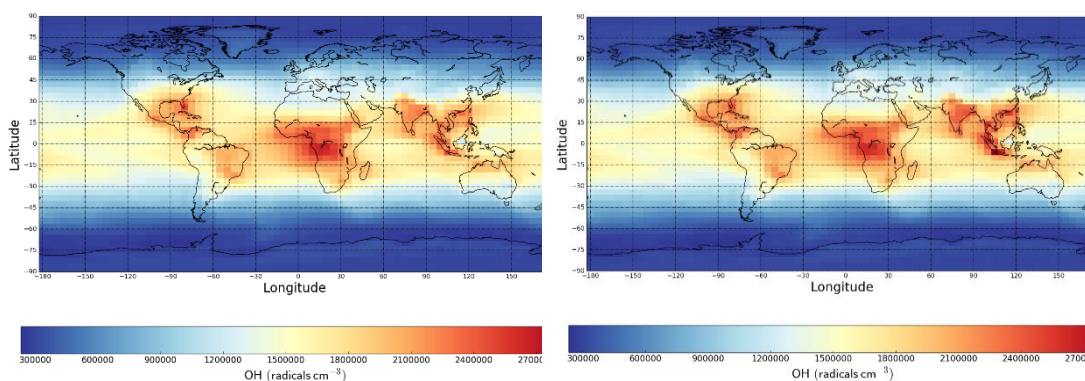


Figure 7.11 C_3H_8 whole column average concentration in 1988 (top left) 2008 (top right) and the change in percentage (left).

7.2.2 Impact on secondary compounds

Figures 7.12 - 7.13 show modelled column averaged concentration of key atmospheric constituents (OH and O_3) between 1988 and 2008. Over this period O_3 concentrations drop slightly ($\sim 2.5\%$) over the northern mid-latitudes reflecting the efforts to control air quality in North America and Europe. Over much of the rest of the world O_3 concentrations have increased (max $\sim 10\%$), driven by the increases in Asia. OH responds in a complicated way to the change in emissions. Over much of the world OH concentrations increase. This increase is notable over Asia, but changes over North America and Europe are also either positive or neutral. Some of this increase reflects an increase in the primary source ($O_3 + h\nu + H_2O$) due to the increased O_3 concentrations. However, over Europe and North America O_3 concentrations have fallen rather than increased. Over these regions the concentrations of OH sinks (NO_x , CO, VOCs) have fallen thus increasing the OH concentration. This has led to an almost universal increase in the OH concentration.



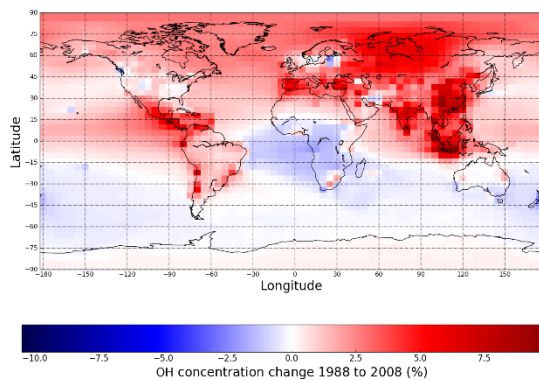


Figure 7.12 OH whole column average concentration in 1988 (top left) 2008 (top right) and the change in percentage (left).

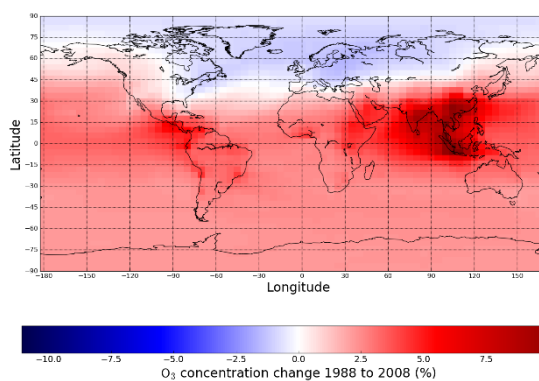
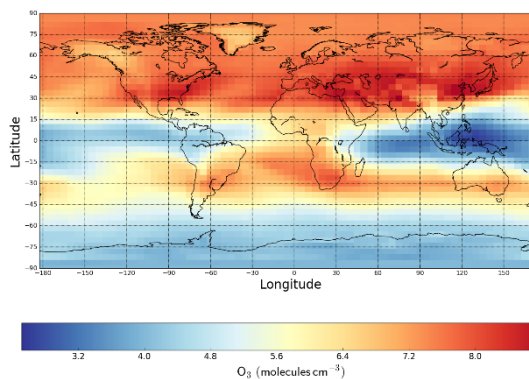
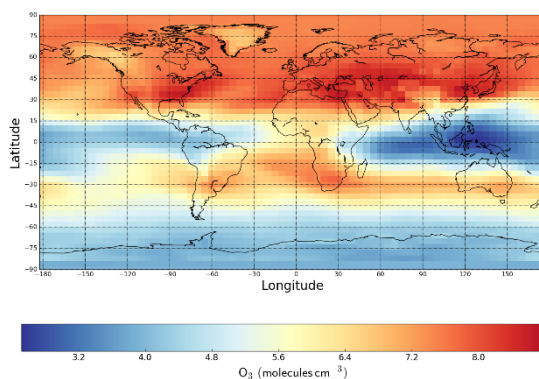


Figure 7.13 O₃ whole column average concentration in 1988 (top left) 2008 (top right) and the change in percentage (left).

7.2.3 Impact on halogenated species.

Figures 7.13 and 7.14 show the column averaged concentration of Cl_{cycling} (Cl, ClOO, HOCl, ClNO₃, ClO, OCIO, Cl₂ and Cl₂O₂) and Cl for 1988 and 2008 and the fractional change. Cl_{cycling} concentrations increase in nearly all locations, most obviously over China, India and South East Asia where Cl_{cycling} concentrations increase by ~30 %. However, all locations increase off the Eastern sea-board of the US and in the tropical Atlantic. Asia has increased production of Cl which is greater than the increased loss due to increase in VOC and CH₄ concentration resulting in a regional net gain of Cl and Cl_{cycling}. America and Europe have seen a decrease in production however due to a greater decreased loss as a result of falling VOC concentrations these areas have actually seen an increase in the Cl. Cl_{cycling} has fallen

over the east coast of America due to the profound (~20 %) drop in NO_x emissions resulting in decreased HOCl.

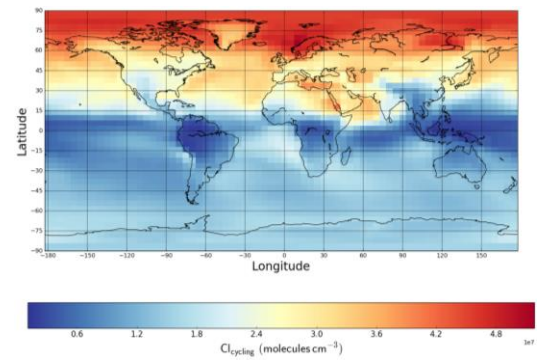
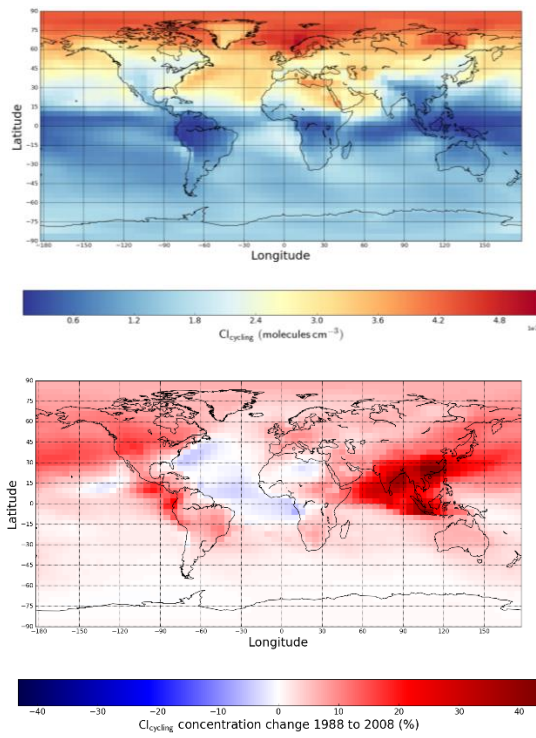


Figure 7.14 Cl_{cycling} whole column average concentration in 1988 (top left) 2008 (top right) and the change in percentage (left).

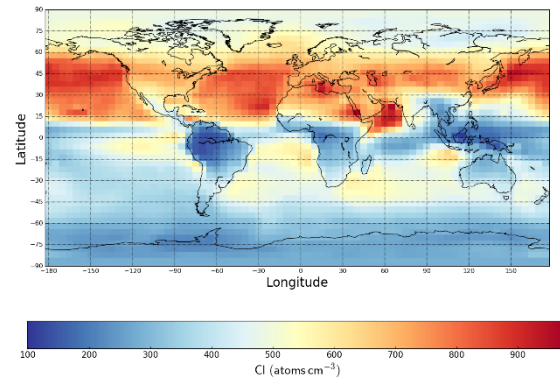
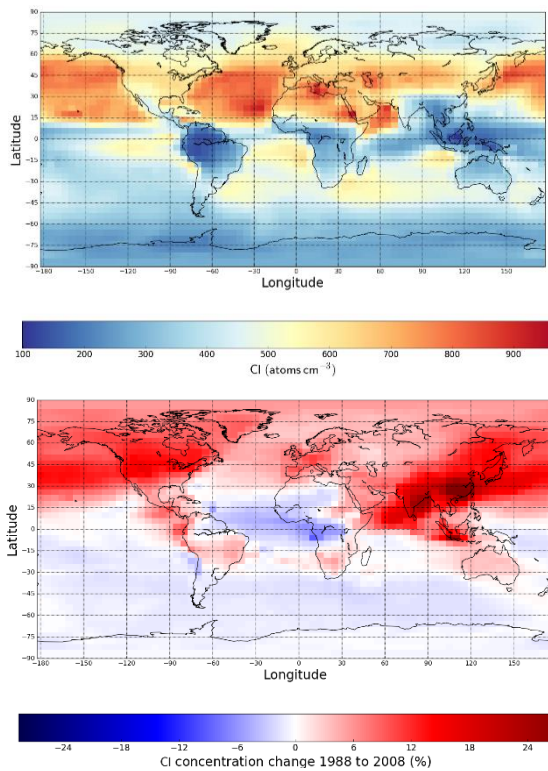


Figure 7.15 atomic Cl whole column average concentration in 1988 (top left) 2008 (top right) and the change in percentage (left).

7.2.4 Impact on Cl / OH removal ratio of ethane

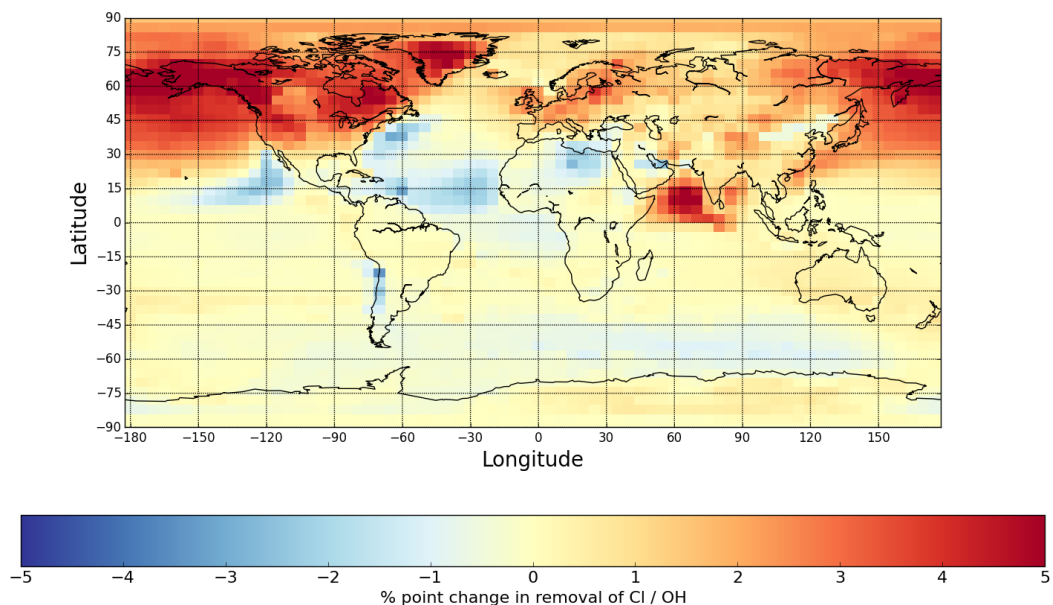


Figure 7.16. Change in ratio of Cl / OH removal ratio between 1998 and 2008.

Figure 7.16 shows that significant changes in the Cl / OH removal ratio have occurred between 1988 and 2008. With much of North America and the Indian ocean seeing a 5-percentage point change in the ratio, this is in line with the witnessed increase in atomic Cl. However much Europe and Asia appear to undergo a more muted change of only a couple of percentage point due to the increased OH in these regions.

7.4 Conclusions

By running simulations with 1998 and 2008 emissions the change in chlorine chemistry between these periods has been explored. The model calculates a significant shift in pollutants over this period with emissions moving from the northern mid-latitude to the tropics. This results in an increases in primary pollutants in the tropics and a reduction in the mid-latitudes. Secondary compounds (O_3 , OH, SO_4^{2-}) respond to these changes resulting in a change in their distribution.

Cl_y and Cl concentrations also change. In general, Cl_y concentrations increase globally due to developing regions experiencing increased Cl production due to increased concentration of NO_x and SO_4^{2-} and developed regions experiencing reduced loss due to decreases in NMVOC emissions. With the exception being Africa which as seen an increase in loss with minimal increase in production.

8. Conclusion

Through this study we have found a global atomic Cl average of 495 cm^{-3} with the the highest concentrations of $1 - 5.5 \times 10^4 \text{ cm}^{-3}$ atomic Cl are found in the tropical marine boundary layer.

Globally the reaction between HOBr and HCl on sulfate aerosol dominates (77 %) the production of Cl precursors through its production of BrCl but in the boundary layer sea-salt sources through reaction with N_2O_5 or iodine species can dominate particularly in polluted regions.

The distribution of reactive chlorine species in the model is complex. Globally the dominant Cl_y species is HCl but in the boundary layer and the northern hemisphere other compounds (notably ClNO_2) can play a significant role in the composition of Cl_y . It is the ultimately the heterogeneous processing which determining the ratio of HCl to more active Cl_y components. Central to this is the rate of removal of Cl to form HCl which essentially determines the lifetime of active chlorine in the atmosphere.

It is evident that, within the model, atomic chlorine can play a role in the oxidizing capacity of the atmosphere. This study supports the theory that the Cl is a small to insignificant CH_4 sink compared to that of OH (0.9 %). However, for ethane and propane, Cl provides a significant sink constituting 15 % and 6.5 % respectively. There is a high degree of regional variability with Cl removal of ethane, with the removal rising over the northern hemisphere oceans to ~ 50 % of OH removal at sea level and ~ 30 % averaged over whole column. In polar regions Cl removal can equal that of OH however in absolute terms the removal is small but it is still notable that in some extreme regions Cl could be the dominant oxidant.

Recent changes in emissions between 1988 and 2008 (NO_x , CO, SO_2 and VOCs) have resulted in Cl concentrations changes. In general, Cl_y concentrations have increased globally due to developing regions experiencing increased Cl production due to increased concentration of NO_x and SO_4^{2-} and developed regions experiencing reduced loss due to decreases in NMVOC concentrations. With the exception being Africa which as seen an increase in loss with minimal increase in production. This offers an interesting feedback loop whereby increased VOCs result in increased removal, and offers interesting potential for further study.

9. References

- ATKINSON, R. 2000. Atmospheric chemistry of VOCs and NO_x. *Atmospheric Environment*, 34, 2063-2101.
- BEY, I., JACOB, D. J., YANTOSCA, R. M., LOGAN, J. A., FIELD, B. D., FIORE, A. M., LI, Q. B., LIU, H. G. Y., MICKLEY, L. J. & SCHULTZ, M. G. 2001. Global modeling of tropospheric chemistry with assimilated meteorology: Model description and evaluation. *Journal of Geophysical Research-Atmospheres*, 106, 23073-23095.
- CARPENTER, L. J., MACDONALD, S. M., SHAW, M. D., KUMAR, R., SAUNDERS, R. W., PARTHIPAN, R., WILSON, J. & PLANE, J. M. C. 2013. Atmospheric iodine levels influenced by sea surface emissions of inorganic iodine. *Nature Geoscience*, 6, 108-111.
- FINLAYSON-PITTS, B. J., KEOSHIAN, C. J., BUEHLER, B. & EZELL, A. A. 1999. Kinetics of reaction of chlorine atoms with some biogenic organics. *International Journal of Chemical Kinetics*, 31, 491-499.
- FINLAYSONPITTS, B. J., EZELL, M. J. & PITTS, J. N. 1989. FORMATION OF CHEMICALLY ACTIVE CHLORINE COMPOUNDS BY REACTIONS OF ATMOSPHERIC NaCl PARTICLES WITH GASEOUS N₂O₅ AND ClONO₂. *Nature*, 337, 241-244.
- GRAEDEL, T. E. & KEENE, W. C. 1996. The budget and cycle of Earth's natural chlorine. *Pure and Applied Chemistry*, 68, 1689-1697.
- HELMIG, D., ROSSABI, S., HUEBER, J., TANS, P., MONTZKA, S. A., MASARIE, K., THONING, K., PLASS-DUELMER, C., CLAUDE, A., CARPENTER, L. J., LEWIS, A. C., PUNJABI, S., REIMANN, S., VOLLMER, M. K., STEINBRECHER, R., HANNIGAN, J., EMMONS, L. K., MAHIEU, E., FRANCO, B., SMALE, D. & POZZER, A. 2016. Reversal of global atmospheric ethane and propane trends largely due to US oil and natural gas production. *Nature Geoscience*, 9, 490-495.
- JAEGLER, L., QUINN, P. K., BATES, T. S., ALEXANDER, B. & LIN, J. T. 2011. Global distribution of sea salt aerosols: new constraints from in situ and remote sensing observations. *Atmospheric Chemistry and Physics*, 11, 3137-3157.
- KEENE, W. C., STUTZ, J., PSZENNY, A. A. P., MABEN, J. R., FISCHER, E. V., SMITH, A. M., VON GLASOW, R., PECHTL, S., SIVE, B. C. & VARNER, R. K. 2007. Inorganic chlorine and bromine in coastal New England air during summer. *Journal of Geophysical Research-Atmospheres*, 112.
- KELLER, C. A., LONG, M. S., YANTOSCA, R. M., DA SILVA, A. M., PAWSON, S. & JACOB, D. J. 2014. HEMCO v1.0: a versatile, ESMF-compliant component for calculating emissions in atmospheric models. *Geoscientific Model Development*, 7, 1409-1417.

- LARY, D. J. 2005. Halogens and the chemistry of the free troposphere. *Atmospheric Chemistry and Physics*, 5, 227-237.
- LAWRENCE, M. G., JOCKEL, P. & VON KUHLMANN, R. 2001. What does the global mean OH concentration tell us? *Atmospheric Chemistry and Physics*, 1, 37-49.
- LIANG, Q., STOLARSKI, R. S., KAWA, S. R., NIELSEN, J. E., DOUGLASS, A. R., RODRIGUEZ, J. M., BLAKE, D. R., ATLAS, E. L. & OTT, L. E. 2010. Finding the missing stratospheric Br-y: a global modeling study of CHBr₃ and CH₂Br₂. *Atmospheric Chemistry and Physics*, 10, 2269-2286.
- MAO, J., FAN, S., JACOB, D. J. & TRAVIS, K. R. 2013. Radical loss in the atmosphere from Cu-Fe redox coupling in aerosols. *Atmospheric Chemistry and Physics*, 13, 509-519.
- O'DOWD, C. D., FACCHINI, M. C., CAVALLI, F., CEBURNIS, D., MIRCEA, M., DECESARI, S., FUZZI, S., YOON, Y. J. & PUTAUD, J. P. 2004. Biogenically driven organic contribution to marine aerosol. *Nature*, 431, 676-680.
- OHARA, T., AKIMOTO, H., KUROKAWA, J., HORII, N., YAMAJI, K., YAN, X. & HAYASAKA, T. 2007. An Asian emission inventory of anthropogenic emission sources for the period 1980-2020. *Atmospheric Chemistry and Physics*, 7, 4419-4444.
- ORDONEZ, C., LAMARQUE, J. F., TILMES, S., KINNISON, D. E., ATLAS, E. L., BLAKE, D. R., SANTOS, G. S., BRASSEUR, G. & SAIZ-LOPEZ, A. 2012. Bromine and iodine chemistry in a global chemistry-climate model: description and evaluation of very short-lived oceanic sources. *Atmospheric Chemistry and Physics*, 12, 1423-1447.
- OSTHOFF, H. D., ROBERTS, J. M., RAVISHANKARA, A. R., WILLIAMS, E. J., LERNER, B. M., SOMMARIVA, R., BATES, T. S., COFFMAN, D., QUINN, P. K., DIBB, J. E., STARK, H., BURKHOLDER, J. B., TALUKDAR, R. K., MEAGHER, J., FEHSENFELD, F. C. & BROWN, S. S. 2008. High levels of nitryl chloride in the polluted subtropical marine boundary layer. *Nature Geoscience*, 1, 324-328.
- PARRELLA, J. P., JACOB, D. J., LIANG, Q., ZHANG, Y., MICKLEY, L. J., MILLER, B., EVANS, M. J., YANG, X., PYLE, J. A., THEYS, N. & VAN ROOZENDAEL, M. 2012. Tropospheric bromine chemistry: implications for present and pre-industrial ozone and mercury. *Atmospheric Chemistry and Physics*, 12, 6723-6740.
- RIEDEL, T. P., BERTRAM, T. H., CRISP, T. A., WILLIAMS, E. J., LERNER, B. M., VLASENKO, A., LI, S. M., GILMAN, J., DE GOUW, J., BON, D. M., WAGNER, N. L., BROWN, S. S. & THORNTON, J. A. 2012. Nitryl Chloride and Molecular Chlorine in the Coastal Marine Boundary Layer. *Environmental Science & Technology*, 46, 10463-10470.

- SANDER, R. 2015. Compilation of Henry's law constants (version 4.0) for water as solvent. *Atmospheric Chemistry and Physics*, 15, 4399-4981.
- SARWAR, G., SIMON, H., XING, J. & MATHUR, R. 2014. Importance of tropospheric ClNO₂ chemistry across the Northern Hemisphere. *Geophysical Research Letters*, 41, 4050-4058.
- SAUERESSIG, G., CROWLEY, J. N., BERGAMASCHI, P., BRUHL, C., BRENNINKMEIJER, C. A. M. & FISCHER, H. 2001. Carbon 13 and D kinetic isotope effects in the reactions of CH₄ with O(D-1) and OH: New laboratory measurements and their implications for the isotopic composition of stratospheric methane. *Journal of Geophysical Research-Atmospheres*, 106, 23127-23138.
- SCHMIDT, J. A., JACOB, D. J., HOROWITZ, H. M., HU, L., SHERWEN, T., EVANS, M. J., LIANG, Q., SULEIMAN, R. M., ORAM, D. E., LE BRETON, M., PERCIVAL, C. J., WANG, S., DIX, B. & VOLKAMER, R. 2016. Modeling the observed tropospheric BrO background: Importance of multiphase chemistry and implications for ozone, OH, and mercury. *Journal of Geophysical Research-Atmospheres*, 121, 11819-11835.
- SHERWEN, T., EVANS, M. J., CARPENTER, L. J., ANDREWS, S. J., LIDSTER, R. T., DIX, B., KOENIG, T. K., SINREICH, R., ORTEGA, I., VOLKAMER, R., SAIZ-LOPEZ, A., PRADOS-ROMAN, C., MAHAJAN, A. S. & ORDONEZ, C. 2016a. Iodine's impact on tropospheric oxidants: a global model study in GEOS-Chem. *Atmospheric Chemistry and Physics*, 16, 1161-1186.
- SHERWEN, T., SCHMIDT, J. A., EVANS, M. J., CARPENTER, L. J., GROSSMANN, K., EASTHAM, S. D., JACOB, D. J., DIX, B., KOENIG, T. K., SINREICH, R., ORTEGA, I., VOLKAMER, R., SAIZ-LOPEZ, A., PRADOS-ROMAN, C., MAHAJAN, A. S. & ORDONEZ, C. 2016b. Global impacts of tropospheric halogens (Cl, Br, I) on oxidants and composition in GEOS-Chem. *Atmospheric Chemistry and Physics*, 16, 12239-12271.
- SHERWEN, T. M., EVANS, M. J., SPRACKLEN, D. V., CARPENTER, L. J., CHANCE, R., BAKER, A. R., SCHMIDT, J. A. & BREIDER, T. J. 2016c. Global modeling of tropospheric iodine aerosol. *Geophysical Research Letters*, 43, 10012-10019.
- THORNTON, J. A., KERCHER, J. P., RIEDEL, T. P., WAGNER, N. L., COZIC, J., HOLLOWAY, J. S., DUBE, W. P., WOLFE, G. M., QUINN, P. K., MIDDLEBROOK, A. M., ALEXANDER, B. & BROWN, S. S. 2010. A large atomic chlorine source inferred from mid-continental reactive nitrogen chemistry. *Nature*, 464, 271-274.
- VESTRENG, V., NTZIACHRISTOS, L., SEMB, A., REIS, S., ISAKSEN, I. S. A. & TARRASON, L. 2009. Evolution of NO_x emissions in Europe with focus on road transport control measures. *Atmospheric Chemistry and Physics*, 9, 1503-1520.

- VOGT, R., CRUTZEN, P. J. & SANDER, R. 1996. A mechanism for halogen release from sea-salt aerosol in the remote marine boundary layer. *Nature*, 383, 327-330.
- VOGT, R., SANDER, R., VON GLASOW, R. & CRUTZEN, P. J. 1999. Iodine chemistry and its role in halogen activation and ozone loss in the marine boundary layer: A model study. *Journal of Atmospheric Chemistry*, 32, 375-395.
- WANG, Y. H., JACOB, D. J. & LOGAN, J. A. 1998. Global simulation of tropospheric O₃-NO_x-hydrocarbon chemistry 1. Model formulation. *Journal of Geophysical Research-Atmospheres*, 103, 10713-10725.
- WAYNE, R. P., POULET, G., BIGGS, P., BURROWS, J. P., COX, R. A., CRUTZEN, P. J., HAYMAN, G. D., JENKIN, M. E., LEBRAS, G., MOORTGAT, G. K., PLATT, U. & SCHINDLER, R. N. 1995. HALOGEN OXIDES - RADICALS, SOURCES AND RESERVOIRS IN THE LABORATORY AND IN THE ATMOSPHERE. *Atmospheric Environment*, 29, 2677-2881.
- WINGENTER, O. W., BLAKE, D. R., BLAKE, N. J., SIVE, B. C., ROWLAND, F. S., ATLAS, E. & FLOCKE, F. 1999. Tropospheric hydroxyl and atomic chlorine concentrations, and mixing timescales determined from hydrocarbon and halocarbon measurements made over the Southern Ocean. *Journal of Geophysical Research-Atmospheres*, 104, 21819-21828.
- WU, S. L., MICKLEY, L. J., JACOB, D. J., LOGAN, J. A., YANTOSCA, R. M. & RIND, D. 2007. Why are there large differences between models in global budgets of tropospheric ozone? *Journal of Geophysical Research-Atmospheres*, 112.
- Scientific Assessment of Ozone Depletion: 2014, World Meteorological Organization, Global Ozone Research and Monitoring Project—*Report No. 55*, 416 pp., Geneva, Switzerland, 2014
- Dlugokencky, E.J., P.M. Lang, A.M. Crotwell, J.W. Mund, M.J. Crotwell, and K.W. Thoning (2016), Atmospheric Methane Dry Air Mole Fractions from the NOAA ESRL Carbon Cycle Cooperative Global Air Sampling Network, 1983 2015, Version: 2016-07-07, ftp://aftp.cmdl.noaa.gov/data/trace_gases/ch4/flask/surface/.